PAPER

Check for updates

Strain correlation functions in isotropic elastic bodies: large wavelength limit for two-dimensional systems

J. P. Wittmer, [ID] * A. N. Semenov [ID] and J. Baschnagel [ID]

Strain correlation functions in two-dimensional isotropic elastic bodies are shown both theoretically (using the general structure of isotropic tensor fields) and numerically (using a glass-forming model system) to depend on the coordinates of the field variable (position vector **r** in real space or wavevector **q** in reciprocal space) and thus on the direction of the field vector and the orientation of the coordinate system. Since the fluctuations of the longitudinal and transverse components of the strain field in reciprocal space are known in the long-wavelength limit from the equipartition theorem, all components of the correlation function tensor field are imposed and no additional physical assumptions are needed. An observed dependence on the field vector direction thus cannot be used as an indication for anisotropy or for a plastic rearrangement. This dependence is different for the associated strain response field containing also information on the localized stress perturbation.

I. Introduction

A. General background

A tensor field assigns a tensor to each point of the mathematical space, in our case for simplicity a two-dimensional Euclidean vector space with Cartesian coordinates and an orthonormal tensor basis.[1–4] Tensor fields are used in differential geometry,[1] general relativity,[5,6] in the analysis of stress and strain in materials[7–9] and in numerous other applications in science and engineering. Tensor fields are experimentally[10,11] or numerically[4,12–32] probed by means of correlation functions[33–35] of their components and, importantly, these correlation functions are themselves components of tensor fields.[4] See Appendix A for a brief review. Assuming translational invariance, correlation functions are naturally best analyzed, both for theoretical[12–14,17] and numerical[4,18,33] reasons, in a first step as functions of the wavevector **q** in reciprocal space. The dependence on the spatial field vector **r** in real space can then be deduced (*cf.* Appendix B) in a second step by inverse Fourier transformation (FT). This was done, *e.g.*, in our recent analysis[4] of the spatial correlations of the (time-averaged) stress tensor fields in amorphous glasses formed by polydisperse Lennard-Jones (pLJ) particles deep in the glass regime (*cf.* Section IIIA). It can thus be shown that all stress correlation functions (both in reciprocal as in real space) can be described by means of one "Invariant Correlation Function" (ICF) in reciprocal space characterizing the typical ensemble

fluctuations of the quenched normal stress components in reciprocal space perpendicular to the wavevector **q**. Under additional but rather general assumptions[4] this ICF is given in the large-wavelength limit by a thermodynamic quantity, the equilibrium Young modulus of the system.

B. Investigated case study

As another example of the general procedure we shall investigate in the present work the correlation functions $c_{\alpha\beta\gamma\delta}(\mathbf{r}) = \mathcal{F}^{-1}[c_{\alpha\beta\gamma\delta}(\mathbf{q})]$ of the instantaneous strain tensor field $\varepsilon_{\alpha\beta}(\mathbf{r})$ in real space. These may be readily obtained[33] from the components of the tensor field

$$c_{\alpha\beta\gamma\delta}(\mathbf{q}) = \langle \varepsilon_{\alpha\beta}(\mathbf{q})\varepsilon_{\gamma\delta}(-\mathbf{q}) \rangle \quad (1)$$

in reciprocal space with $\varepsilon_{\alpha\beta}(\mathbf{q}) = \mathcal{F}[\varepsilon_{\alpha\beta}(\mathbf{r})]$ being the Fourier transformed strain tensor field components. (The average $\langle \ldots \rangle$ will be specified below) An example for the autocorrelation function $c_{1212}(\mathbf{r})$ of the shear strain $\varepsilon_{12}(\mathbf{r})$ is given in Fig. 1 for the same two-dimensional model system already used in ref. 4 and 18. Interestingly, the correlation function is seen to strongly depend both on the orientation of the field vector **r** (panel (a)) and on the rotation angle α of the coordinate system (panel (b)). Since the simulated system can be shown to be perfectly isotropic down to a few particle diameters,[4,18,36–39] these findings beg for an explanation. Expanding on our recent work on stress correlations,[4,17,18] this behavior can be traced back to the fact that correlation functions of tensor fields of isotropic systems must be components of a generic isotropic

Institut Charles Sadron, Université de Strasbourg & CNRS, 23 rue du Loess, 67034 Strasbourg Cedex, France. E-mail: joachim.wittmer@ics-cnrs.unistra.fr
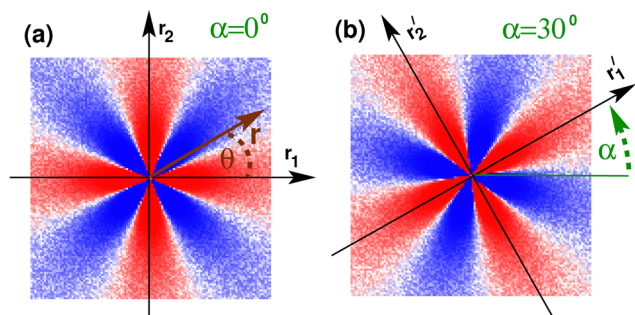
Fig. 1 Autocorrelation function $c_{1212}(\mathbf{r})$ of the strain field component $\varepsilon_{12}(\mathbf{r})$ obtained from our colloidal glasses in two dimensions: (a) unrotated frame with coordinates (r_1, r_2), (b) frame (r_1', r_2') rotated by an angle $\alpha = 30°$ (rotations marked by "'"). Albeit the system is isotropic, the correlation function is strongly angle dependent, revealing an octupolar symmetry. While each pixel corresponds in (a) and (b) to the same spatial position $\mathbf{r}$, the correlation functions differ by the angle α. $c_{1212}(\mathbf{r})$ is positive (red) along the axes and negative (blue) along the bisection lines of the respective axes.

tensor field (*cf.* Section IIB). This field is shown below (*cf.* Section IIID) to be completely described in terms of two ICFs $c_L(q)$ and $c_T(q)$ in reciprocal space ($q = |\mathbf{q}|$ being the magnitude of the wavevector). These ICFs characterize the independent fluctuations of the longitudinal and transverse strain components $\varepsilon_L(\mathbf{q})$ and $\varepsilon_T(\mathbf{q})$. Due to the equipartition theorem of statistical physics $c_L(q)$ and $c_T(q)$ are given by[7,10,11,21]

$$\beta V c_L(q) \to \frac{1}{\lambda + 2\mu} \text{ and } \beta V c_T(q) \to \frac{1}{4\mu} \text{ for } q \to 0 \quad (2)$$

in the large-wavelength limit with $\beta = 1/k_B T$ being the inverse temperature, V the d-dimensional volume of the system and λ and μ two macroscopic Lamé coefficients.[7,8] All strain correlation functions are thus imposed on large scales. In turn this explains without any additional physical input the octupolar pattern† observed in Fig. 1 (*cf.* Section IVC and Appendix D) and shows that strain correlations in elastic bodies must necessarily be long-ranged. This is different for the closely related but distinct tensorial response field being the tensorial product of correlation functions and the imposed tensorial perturbation. As emphasized in Sections IIE and V, the response field thus contains additional information due to the source term and its symmetry.

C. Outline

We begin in Section II with some general theoretical considerations on isotropic tensor fields. Technical points concerning the model system and the data production of tensorial fields on discrete grids are discussed in Section III. This is followed in Section IV by the presentation of our main numerical results. The strain response due to an imposed stress point source is discussed in Section V. A summary and an outlook are given in

---

† See, *e.g.*, the wikipedia entries on quadrupoles and general multipolar expansions as used, say, in electrostatics. For the planar harmonic basis functions $\cos(p\theta)$ or $\sin(p\theta)$ a monopole corresponds to $p = 0$, a dipole to $p = 1$, a quadrupole to $p = 2$ and an octupole to $p = 4$.

Section VI. More details may be found in the Appendix both on the theoretical background (*cf.* Appendices A and D) and on computational issues (*cf.* Appendices B and C).

II. General considerations

A. Isotropic tensors and tensor fields

Isotropic systems, such as generic isotropic elastic bodies,[7–9] simple and complex fluids,[34,40–42] amorphous metals and glasses,[23–25,27–32,43] polymer networks and gels,[40,41] foams and emulsions[20,22] or, as a matter of fact, our entire universe[5] are described at least on some scales by isotropic tensors and isotropic tensor fields (*cf.* Appendix A2).[1,3,9] It is well known[3,9] that the components of isotropic tensors remain unchanged under an orthogonal coordinate transformation (including rotations and reflections). For instance,

$$E^*_{\alpha\beta\gamma\delta} = E_{\alpha\beta\gamma\delta} \quad (3)$$

for the forth-order elastic modulus tensor of an isotropic body (*cf.* Appendix C3)[8,9] with "*" marking an arbitrary orthogonal transformation (*cf.* Appendix A1). This implies (*cf.* Appendix A4) that $E_{\alpha\beta\gamma\delta}$ is given by two invariants, *e.g.*, the two Lamé coefficients λ and μ. Importantly, this does not hold for isotropic tensor fields.[3,4,17] For instance, for a forth-order correlation function in reciprocal space the isotropy condition becomes

$$c^*_{\alpha\beta\gamma\delta}(\mathbf{q}) = c_{\alpha\beta\gamma\delta}(\mathbf{q}^*) \quad (4)$$

with $\mathbf{q}^*$ being the "actively" transformed wavevector (*cf.* Appendix A2).

B. Structure of isotropic correlation functions

Assuming in addition the system to be achiral and two-dimensional (*cf.* Appendix A3) it can be shown[4] that correlation functions of second-order tensor field components must take the following mathematical structure

$$
\begin{aligned}
c_{\alpha\beta\gamma\delta}(\mathbf{q}) &= i_1(q)\delta_{\alpha\beta}\delta_{\gamma\delta} \\
&+ i_2(q)\big[\delta_{\alpha\gamma}\delta_{\beta\delta} + \delta_{\alpha\delta}\delta_{\beta\gamma}\big] \\
&+ i_3(q)\big[\hat{q}_\alpha\hat{q}_\beta\delta_{\gamma\delta} + \hat{q}_\gamma\hat{q}_\delta\delta_{\alpha\beta}\big] \\
&+ i_4(q)\hat{q}_\alpha\hat{q}_\beta\hat{q}_\gamma\hat{q}_\delta
\end{aligned}
\quad (5)
$$

in terms of four ICFs $i_n(q)$, the coordinates $\hat{q}_\alpha$ of the normalized wavevector $\hat{\mathbf{q}}$ and the Kronecker symbol $\delta_{\alpha\beta}$. Legitimate correlation functions of isotropic systems may thus depend on $\hat{q}_\alpha$ and, hence, on the orientation of the wavevector and of the coordinate system. While the isotropy of the system may not be manifested by *one* correlation function, it is crucial for the structure of the complete set of all correlation functions given by eqn (5). We note finally that it is useful to express the above ICFs in terms of an alternative set of ICFs $c_L(q)$, $c_T(q)$, $c_\perp(q)$ and

$c_N(q)$ given by

$$i_1(q) = c_N(q) - 2c_T(q)$$
$$i_2(q) = c_T(q)$$
$$i_3(q) = c_\perp(q) - c_N(q) + 2c_T(q) \qquad (6)$$
$$i_4(q) = c_L(q) + c_N(q) - 2c_\perp(q) - 4c_T(q).$$

See Appendix A4 for more details.

C. Planar harmonic basis functions

Instead of using the components $\hat{q}_\alpha$ one may, quite generally, express all isotropic tensor fields in two dimensions in terms of the orthogonal planar harmonic basis functions $\cos(p\theta)$ and $\sin(p\theta)$ with $\hat{q}_1 = \cos(\theta)$ and $\hat{q}_2 = \sin(\theta)$ and $p = 0$, 2 and 4. (See Appendix D for more details.) For instance, it follows from eqn (5) that

$$c_{1212}(\mathbf{q}) = i_2(q) + \frac{i_4(q)}{8} - \frac{i_4(q)}{8}\cos(4\theta). \qquad (7)$$

Hence, if the invariant $i_4(q)$ is sufficiently large, $c_{1212}(\mathbf{q})$ must reveal an octupolar pattern. Due to eqn (B18) derived in Appendix B3, this alternative representation is especially useful for performing the inverse FT to real space. This also shows that the corresponding correlation function $c_{\alpha\beta\gamma\delta}(\mathbf{r}) = \mathcal{F}^{-1}[c_{\alpha\beta\gamma\delta}(\mathbf{q})]$ in real space must have the same mathematical properties.

D. Response to point source

Let us consider the second order tensor field $R_{\alpha\beta}(\mathbf{q})$ obtained by the contraction

$$R_{\alpha\beta}(\mathbf{q}) = \frac{1}{V}c_{\alpha\beta\gamma\delta}(\mathbf{q})s_{\gamma\delta} \qquad (8)$$

with a symmetric but not necessarily isotropic tensor $s_{\alpha\beta}$ using the standard summation convention over repeated indices.[1,3] (For convenience we have introduced the system volume V.) We shall call $R_{\alpha\beta}(\mathbf{q})$ the "response field" (in reciprocal space) and $s_{\alpha\beta}$ the "point source tensor". In fact, using eqn (B4) and (B6) it is seen that in real space the tensor $s_{\alpha\beta}/V$ corresponds to a "point source" $s_{\alpha\beta}\delta(\mathbf{r})$ (using Dirac's delta function) and $R_{\alpha\beta}(\mathbf{q})$ becomes

$$R_{\alpha\beta}(\mathbf{r}) = \mathcal{F}^{-1}[R_{\alpha\beta}(\mathbf{q})] = c_{\alpha\beta\gamma\delta}(\mathbf{r})s_{\gamma\delta} \qquad (9)$$

using $c_{\alpha\beta\gamma\delta}(\mathbf{r}) = \mathcal{F}^{-1}[c_{\alpha\beta\gamma\delta}(\mathbf{q})]$. We shall say more about the specific linear strain response in real space in Section V but focus here on the generic response in reciprocal space. Being symmetric the source tensor may be diagonalized by a rotation of the coordinate system where $s_{12} = s_{21} = 0$ and s_{11} and s_{22} become the two (in general not identical) eigenvalues. Hence,

$$R_{\alpha\beta}(\mathbf{q}) = \frac{1}{V}[s_{11}c_{\alpha\beta11}(\mathbf{q}) + s_{22}c_{\alpha\beta22}(\mathbf{q})]. \qquad (10)$$

We emphasize that the sum must be taken over all eigenvalues of the source tensor, *i.e.* two for the presented two-dimensional case. (The failure to sum properly over all tensorial contributions to $R_{\alpha\beta}(\mathbf{q})$ leads to incorrect angular dependences.) Importantly,

$R_{\alpha\beta}(\mathbf{q})$ thus contains information over both the system, characterized by the correlation functions, and the imposed source term.

E. Different types of source terms

If we now assume that not only $c_{\alpha\beta\gamma\delta}(\mathbf{q})$ is an isotropic tensor field but that, moreover, $s_{\alpha\beta}$ is isotropic, *i.e.* $s_{11} = s_{22}$, the product theorem eqn (A7) discussed in Appendix A2 implies that $R_{\alpha\beta}(\mathbf{q})$ must also be an isotropic tensor field. According to eqn (A15) it is given by

$$R_{\alpha\beta}(\mathbf{q}) = k_1(q)\delta_{\alpha\beta} + k_2(q)\hat{q}_\alpha\hat{q}_\beta \qquad (11)$$

in terms of two invariants $k_1(q)$ and $k_2(q)$ which can in turn be expressed in terms of the invariants of $c_{\alpha\beta\gamma\delta}(\mathbf{q})$ and $s_{\alpha\beta}$. $R_{\alpha\beta}(\mathbf{q})$ can thus at most be quadrupolar ($p = 2$). Specifically,

$$R_{12}(\mathbf{q}) = k_2(q)\hat{q}_1\hat{q}_2 \propto \sin(2\theta) \qquad (12)$$

which is distinct from $c_{1212}(\mathbf{q})$, *cf.* eqn (7). Importantly, in many physical situations the source is in fact *not* isotropic and thus in turn the response field not consistent with eqn (11). We remind that according to a popular model of localized plastic failure by means of "shear transformation zones"[23,44–47] two orthogonal twin force dipoles of opposite signs may be imposed at the origin.‡ This suggests to consider the case $s_{11} = -s_{22}$. It follows then from eqn (5) and (10) that

$$R_{12}(\mathbf{q}) \propto i_4(q)\hat{q}_1\hat{q}_2(\hat{q}_1^2 - \hat{q}_2^2) \propto \sin(4\theta). \qquad (13)$$

The (non-isotropic) response field $R_{12}(\mathbf{q})$ thus is in this case octupolar as the correlation field $c_{1212}(\mathbf{q})$, however, shifted by an angle $\pi/8$. It is readily seen by inverse FT that the same general behavior applies in real space.

III. Technical issues

A. Algorithm, configurations and frames

We investigate amorphous glasses in two dimensions formed by pLJ particles[4,18,36–39,48] which are sampled by means of Monte Carlo (MC) simulations.[33] See Appendix C for details (Hamiltonian, units, cooling and equilibration procedure, data production, generation and analysis of tensor fields on discrete grids). We focus on systems containing $n = 10\,000$ and $40\,000$ particles at a working temperature $T = 0.2$. This is much lower than the glass transition temperature $T_g \approx 0.26$,[36] *i.e.* for any computationally feasible production time the systems behave as solid elastic bodies.[38] $N_c = 200$ completely independent configurations c are prepared using a mix of local and swap MC hopping moves[38,49] while the presented data are computed using local MC moves only. For each c we store time-series containing $N_t = 10\,000$ "frames" t computed using equidistant time intervals. As described in Appendix C3, the elastic modulus tensor is isotropic and determined by the two Lamé coefficients $\lambda \approx 38$ and $\mu \approx 14$.[36,38]

---

‡ Let us impose in a rotated coordinate system at $\alpha = -\pi/4$ a symmetric source tensor with a finite "shear" $s'_{12} = s$ and vanishing diagonal components $s'_{11} = s'_{22} = 0$. Using eqn (A2) this implies $S_{11} = -S_{22} = s$ and $S_{12} = 0$ in the original coordinate system at $\alpha = 0$.

B. Sampled discrete tensorial fields

As shown in Fig. 2, a discrete square grid is used to store and to manipulate the various fields needed for the microscopic description. The standard lattice constant for the grid in real space is $a_{grid} \approx 0.2$. The displacement field $\mathbf{u}(\mathbf{r})$ in real space is determined for each frame t using a standard method[10,11,21] from the displacement vector of each particle using as reference position the time-averaged particle position (*cf.* Appendix C5). We obtain then from the Fourier transformed displacement field $\mathbf{u}(\mathbf{q}) = \mathcal{F}[\mathbf{u}(\mathbf{r})]$ the strain tensor field[8,17]

$$\varepsilon_{\alpha\beta}(\mathbf{q}) = \frac{i}{2}(q_\beta u_\alpha(\mathbf{q}) + q_\alpha u_\beta(\mathbf{q})) \tag{14}$$

in reciprocal space. Using the correlation function theorem for FTs (*cf.* Appendix B) the strain correlations functions in reciprocal space are given by eqn (1) where the average is taken over all t and c. Both strain and correlation function fields in reciprocal space are defined to be dimensionless (*cf.* Appendix B1). We emphasize by a prime "'" all tensor field components obtained in a coordinate system rotated by an angle α (with $\alpha = 0$ being the original unrotated system). Specifically, the correlation functions $c'_{\alpha\beta\gamma\delta}(\mathbf{q}) = \langle\varepsilon'_{\alpha\beta}(\mathbf{q})\varepsilon'_{\gamma\delta}(-\mathbf{q})\rangle$ are obtained using the components $u'_\alpha(\mathbf{r})$ and q'_α in the rotated frame.

C. Natural Rotated Coordinates

All the tensorial fields introduced above depend on the orientation of the coordinate system. Importantly, we consider these properties in a first step in "Natural Rotated Coordinates" (NRC) where for each wavevector $\mathbf{q}$ the coordinate system is rotated until the 1-axis coincides with the $\mathbf{q}$-direction. We mark these new tensor field components by "∘" to distinguish them from standard rotated tensor field components (marked by primes "'"). Note that $q_\alpha^\circ = q\delta_{1\alpha}$ for all wavevectors $\mathbf{q}$. Using the

components q_α° and $u_\alpha^\circ(\mathbf{q})$ we obtain (as before) the strain tensor $\varepsilon_{\alpha\beta}^\circ(\mathbf{q})$. Importantly,

$$q_2^\circ = 0 \Rightarrow \varepsilon_{22}^\circ(\mathbf{q}) = 0 \tag{15}$$

in agreement with eqn (14). We thus only have two independent components of the strain tensor field in NRC. We alternatively write for convenience $u_L(\mathbf{q}) \equiv u_1^\circ(\mathbf{q})$, $u_T(\mathbf{q}) \equiv u_2^\circ(\mathbf{q})$, $\varepsilon_L(\mathbf{q}) \equiv \varepsilon_{11}^\circ(\mathbf{q})$ and $\varepsilon_T(\mathbf{q}) \equiv \varepsilon_{12}^\circ(\mathbf{q}) \equiv \varepsilon_{21}^\circ(\mathbf{q})$ for the longitudinal and transverse components of the displacement and strain tensor fields. Note that

$$\varepsilon_{11}^\circ(\mathbf{q}) \equiv \varepsilon_L(\mathbf{q}) = iqu_L(\mathbf{q}) \tag{16}$$

and

$$\varepsilon_{12}^\circ(\mathbf{q}) \equiv \varepsilon_{21}^\circ(\mathbf{q}) \equiv \varepsilon_T(\mathbf{q}) = iqu_T(\mathbf{q})/2, \tag{17}$$

i.e. displacement and strain fields in NRC contain essentially the same information.

D. Correlation functions in NRC

The correlation functions $c_{\alpha\beta\gamma\delta}^\circ(\mathbf{q}) \equiv \langle\varepsilon_{\alpha\beta}^\circ(\mathbf{q})\varepsilon_{\gamma\delta}^\circ(-\mathbf{q})\rangle$ may for finite N_c not only depend on q but also on $\hat{\mathbf{q}}$. Consistently with eqn (A18) and ref. 4, 17 and 18 we thus operationally define the ICFs $c_L(q) \equiv \langle c_{1111}^\circ(\mathbf{q})\rangle_{\hat{\mathbf{q}}}$, $c_T(q) \equiv \langle c_{1212}^\circ(\mathbf{q})\rangle_{\hat{\mathbf{q}}}$, $c_N(q) \equiv \langle c_{2222}^\circ(\mathbf{q})\rangle_{\hat{\mathbf{q}}}$ and $c_\perp(q) \equiv \langle c_{1122}^\circ(\mathbf{q})\rangle_{\hat{\mathbf{q}}}$ by averaging over all wavevectors with $|\mathbf{q}| \approx q$. However, $\varepsilon_{22}^\circ(\mathbf{q}) = 0$ implies immediately that

$$c_{2222}^\circ(\mathbf{q}) = c_{1122}^\circ(\mathbf{q}) = c_N(q) = c_\perp(q) = 0 \text{ for } \forall\mathbf{q}. \tag{18}$$

The two remaining non-trivial ICFs $c_L(q)$ and $c_T(q)$ are called, respectively, the "longitudinal ICF" and the "transverse ICF". As already noted in the Introduction, according to the equipartition theorem $c_L(q)$ and $c_T(q)$ are given for sufficiently large wavelengths by the Lamé coefficients λ and μ. The stated eqn (2) can be readily obtained from published work[7,10,11,21] using eqn (16) and (17) to substitute the displacement fields $u_L(\mathbf{q})$ and $u_T(\mathbf{q})$ in NRC by the corresponding strain fields $\varepsilon_L(\mathbf{q})$ and $\varepsilon_T(\mathbf{q})$.

IV. Main numerical results

A. Measured longitudinal and transverse ICFs

We turn now to the numerical results of this work. Fig. 3 focuses on the two non-vanishing correlation functions obtained in reciprocal space and NRC. All correlation functions are rescaled by βV having thus the dimension of an inverse modulus. As can be seen for the two indicated particle numbers n, a data collapse for different system sizes is observed, confirming the expected volume scaling. The inset presents the (not yet spherically averaged) correlation functions $\beta V c_{1212}^\circ(\mathbf{q})$ and $\beta V c_{1111}^\circ(\mathbf{q})$ as functions of the wavevector angle θ for one small wavevector with $q \approx 0.1$. As expected for isotropic systems, these correlation functions are θ-independent (apart from a small noise contribution due to the finite number of independent configurations). The main panel presents the $\hat{\mathbf{q}}$-averaged longitudinal and transverse ICFs $\beta V c_L(q)$ and $\beta V c_T(q)$ as functions of q. The expected large-wavelength limit
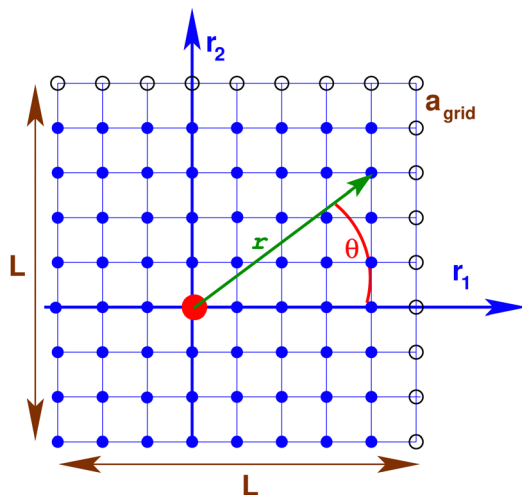

Fig. 2 Two-dimensional ($d = 2$) square lattice with a_{grid} being the lattice constant and $n_L = L/a_{grid}$ the number of grid points in one spatial dimension. The filled circles indicate microcells of the principal box, the open circles some periodic images. The spatial position $\mathbf{r}$ of a microcell is either given by the r_1- and r_2-coordinates (in the principal box) or by the distance $r = |\mathbf{r}|$ from the origin (large circle) and the angle θ.
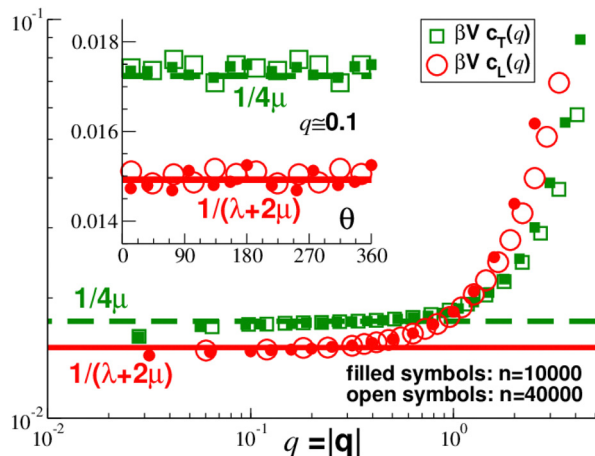
Fig. 3 Rescaled correlation functions in NRC and reciprocal space. The bold dashed and solid lines indicate the expected low-q limit eqn (2). Inset: $\beta V c_{1212}^{o}(\mathbf{q})$ and $\beta V c_{1111}^{o}(\mathbf{q})$ vs. θ for $q \approx 0.1$. Main panel: Semi-logarithmic representation of ICFs $\beta V c_T(q)$ and $\beta V c_L(q)$ vs. q.
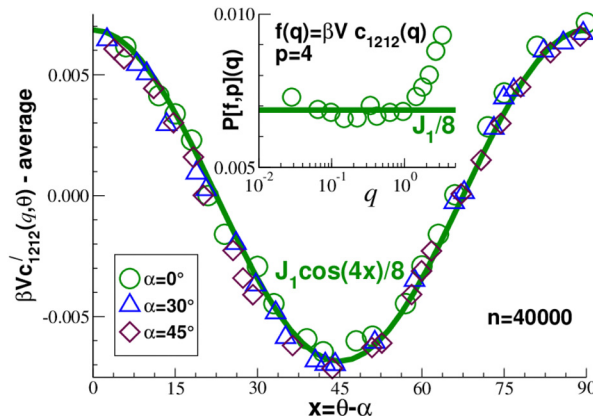

Fig. 4 Rescaled correlation function $f(\mathbf{q}) = \beta V c_{1212}^{'}(\mathbf{q})$ for $n = 40\,000$. Main panel: Angle dependence of vertically shifted $f(\mathbf{q})$ for $q \approx 0.1$. Data collapse is observed using the reduced angle $x = \theta - \alpha$. The bold solid line indicates the prediction, eqn (20). Inset: Comparison of $P[f,p](q)$ for $p = 4$ with the predicted low-q limit $J_1/8$ (bold solid line).

eqn (2) is indicated in both panels by bold horizontal lines. As can be seen in the main panel, it is well confirmed for $q \ll 1$ over at least one order of magnitude where we have used the known values of λ and μ. We remind that eqn (2) has been used in various experimental and numerical studies[10,11,21] to fit λ and μ. $c_L(q)$ and $c_T(q)$ characterize the typical length of the complex random variables $\varepsilon_L(\mathbf{q})$ and $\varepsilon_T(\mathbf{q})$. Their distributions and correlations will be discussed elsewhere.[50] We note finally that the increase of the ICFs from the low-q asymptotics visible for $q > 1$ correlates with the deviation of the total static structure factor $S(q)$ from its low-q plateau (cf. Fig. 6).

B. Correlation functions in reciprocal space

While remaining in reciprocal space we consider next coordinate frames which are either unrotated ($\alpha = 0$) or rotated as in Fig. 1(b) using the *same* angle α for all $\mathbf{q}$. According to eqn (5) the correlation functions $c_{\alpha\beta\gamma\delta}(\mathbf{q})$ of isotropic achiral systems in two dimensions depend quite generally on the four ICFs $c_L(q)$, $c_T(q)$, $c_N(q)$ and $c_\perp(q)$. Due to eqn (18) the last two of these ICFs must vanish while $c_L(q)$ and $c_T(q)$ are given by eqn (2). Let us introduce for later convenience the two "creep compliances"

$$J_1 \equiv \frac{1}{\mu} - \frac{1}{\lambda + 2\mu} \text{ and } J_2 \equiv \frac{2}{\lambda + 2\mu}. \quad (19)$$

This yields in the original coordinates

$$\beta V c_{1212}(\mathbf{q}) \to \frac{J_1}{8}\cos(4\theta) + \ldots \quad (20)$$

$$\beta V c_{1122}(\mathbf{q}) \to \frac{J_1}{8}\cos(4\theta) + \ldots \quad (21)$$

$$-\frac{\beta V}{2}(c_{1111}(\mathbf{q}) + c_{2222}(\mathbf{q})) \to \frac{J_1}{8}\cos(4\theta) + \ldots \quad (22)$$

$$\frac{\beta V}{2}(c_{1111}(\mathbf{q}) - c_{2222}(\mathbf{q})) \to \frac{J_2}{4}\cos(2\theta) + \ldots \quad (23)$$

for $q \to 0$. The dots mark irrelevant constant contributions.§ See Appendix D for more details. For correlation functions $c_{\alpha\beta\gamma\delta}^{'}(\mathbf{q})$ in rotated coordinate systems one merely needs to substitute θ by $x = \theta - \alpha$. These relations are put to a test in Fig. 4 where we focus for clarity on the reduced shear-strain autocorrelation function $f(\mathbf{q}) = \beta V c_{1212}^{'}(\mathbf{q})$ for $n = 40\,000$. The angular dependences are presented in the main panel for one wavevector in the low-q limit. Focusing on the first term in eqn (20) we have taken off the mean constant average over all θ (corresponding to the dots). Importantly, all data for different α are seen to collapse when plotted as a function of the scaling variable x. Obviously, this simple scaling (without characteristic angle) would not hold for anisotropic systems. To obtain a precise test of the q-dependence of $c_{\alpha\beta\gamma\delta}(\mathbf{q})$ we project out the angular dependences using

$$P[f,p](q) \equiv 2 \times \frac{1}{2\pi}\int_0^{2\pi} d\theta f(q,\theta)\cos(p\theta) \quad (24)$$

for $p = 2$ and $p = 4$. For convenience the prefactor of the integral is chosen such that $P[\cos(2\theta),2] = P[\cos(4\theta),4] = 1$. The result for the shear-stress autocorrelation function with $p = 4$ is shown in the inset of Fig. 4. In agreement with eqn (20) the presented data is given by $J_1/8$ (solid line) for sufficiently small wavevectors. Equivalent results have been obtained for the other correlation functions mentioned above.

C. Correlation functions in real space

We turn finally to the correlation functions $c_{\alpha\beta\gamma\delta}^{'}(\mathbf{r}) = \mathcal{F}^{-1}[c_{\alpha\beta\gamma\delta}^{'}(\mathbf{q})]$ in real space. As shown in Appendix D, inverse

§ The omitted constant terms correspond to localized $\delta(\mathbf{r})$ contributions to strain correlation functions in real space. For example, such a contribution to $c_{1212}(\mathbf{r})$ is $\frac{J_1 + J_2}{8\beta}\delta(\mathbf{r})$.
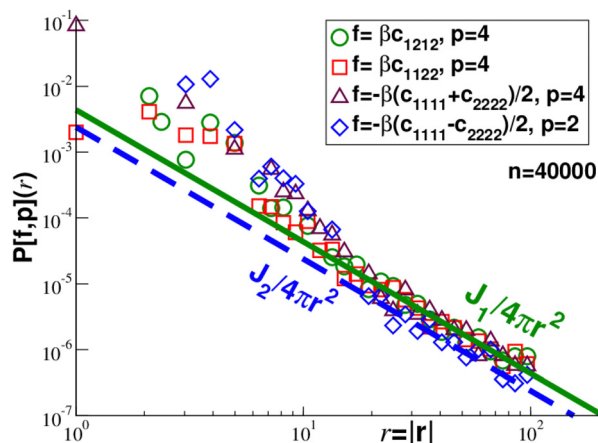
Fig. 5 $P[f,p](r)$ for various correlation functions and modes p for $n = 40\,000$. The bold solid line marks the prediction $J_1/4\pi r^2$ for the first three cases, the dashed line the prediction $J_2/4\pi r^2$ for the last one.

FT implies

$$\beta c'_{1212}(\mathbf{r}) \simeq \frac{J_1}{4\pi r^2}\cos(4x) \text{ for } r \gg 1 \quad (25)$$

with $x = \theta - \alpha$ being the difference of the angles θ and α indicated in Fig. 1. The same large-r limit holds also for $\beta c'_{1122}(r)$ and for $-\beta(c'_{1111}(r) + c'_{2222}(r))/2$. Moreover,

$$\beta(c'_{1111}(r) - c'_{2222}(r))/2 \simeq -\frac{J_2}{4\pi r^2}\cos(2x) \quad (26)$$

for $r \gg 1$, *i.e.* a dipolar symmetry is expected. A verification of the r-dependence is obtained using again (now in real space) the projection $P[f,p](r)$, *cf.* eqn (24). Focusing on $n = 40\,000$ several rescaled correlation functions $f(\mathbf{r})$ are presented in Fig. 5. In agreement with eqn (25) the indicated first three cases collapse for $p = 4$ and $r \gtrsim 20$ on $J_1/4\pi r^2$ (bold solid line). This confirms the octupolar symmetry of these correlation functions. Confirming eqn (26) the last case with $f(\mathbf{r}) = -\beta(c_{1111}(\mathbf{r}) - c_{2222}(\mathbf{r}))/2$ collapses onto $J_2/4\pi r^2$ (dashed line). $p = 2$ is used here in agreement with the predicted quadrupolar symmetry of this correlation function. Similar results are obtained for other particle numbers n.

V. Linear response to point stress

A. Time-dependent strain correlations

Correlation functions describe quite generally the linear response to a small imposed perturbation.[7,34,35,42] Being tensorial fields, just like the correlation function fields, the response fields must in general depend on the direction of the field vector and on the orientation of the coordinate system. As already emphasized in Section II4 and Section II5, the response fields contains information of both the system and the imposed source and the source term may either be isotropic or anisotropic. We elaborate here this general point focusing, naturally, on correlation functions of the instantaneous strain field $\hat{\varepsilon}_{\alpha\beta}(\mathbf{r}) = \varepsilon_{\alpha\beta}(\mathbf{r}, t)$. Extending very briefly our discussion to the

time domain, let us introduce the time-dependent correlation functions

$$c_{\alpha\beta\gamma\delta}(\mathbf{q}, t) = \langle \varepsilon_{\alpha\beta}(\mathbf{q}, t)\varepsilon_{\gamma\delta}(-\mathbf{q}, t = 0) \rangle \quad (27)$$

of the strain fields in reciprocal space with t being the "time lag".[33] Naturally, this reduces to eqn (1) for $t \to 0$. This definition allows us to take advantage of the general "Fluctuation-dissipation theorem" (FDT) of statistical mechanics as stated, *e.g.*, in ref. 34, 35 and 42. We thus anticipate immediate generalizations of the present study for time-dependent tensorial correlation and response fields which will be discussed elsewhere.

B. Fluctuation-dissipation theorem

Let us switch on at time $t = 0$ a small perturbation

$$\Delta\mathcal{H} = -\int d\mathbf{r}\,\delta\sigma_{\alpha\beta}(\mathbf{r})\hat{\varepsilon}_{\alpha\beta}(\mathbf{r}) \text{ for } t \geq 0 \quad (28)$$

to the Hamiltonian $\Delta\mathcal{H} = \mathcal{H}_0 + \Delta\mathcal{H}$ of the system with $\delta\sigma_{\alpha\beta}(\mathbf{r})$ being an imposed external stress field. This is equivalent to the application of an appropriate external perturbative force field to each particle. For a general "growth function"[42] in response to a sudden application of a step field, such as eqn (28), the relevant FDT relations are stated (for scalar fields) by eqn (3.65) and (3.67) of ref. 42. The mean strain increment $\delta\varepsilon_{\alpha\beta}(\mathbf{r}, t)$ induced by this perturbation is then given in real space by a convolution integral for the time-dependent correlation functions $c_{\alpha\beta\gamma\delta}(\mathbf{r}, t)$ and the stress perturbation $\delta\sigma_{\alpha\beta}(\mathbf{r})$. Using eqn (B6) this relation may be written more compactly in reciprocal space as

$$\delta\varepsilon_{\alpha\beta}(\mathbf{q}, t) = \beta V \left[c_{\alpha\beta\gamma\delta}(\mathbf{q}, t = 0) - c_{\alpha\beta\gamma\delta}(\mathbf{q}, t) \right]\delta\sigma_{\gamma\delta}(\mathbf{q}) \quad (29)$$

where the summation over repeated indices is essential and cannot be omitted. Note that $\delta\varepsilon_{\alpha\beta}(\mathbf{q}, t) = 0$ for $t \leq 0$ and that, since all $c_{\alpha\beta\gamma\delta}(\mathbf{q}, t)$ are continuous functions of time, the creep response $\delta\varepsilon_{\alpha\beta}(\mathbf{q}, t)$ must also be continuous, especially at $t = 0$.[40] The time-dependent creep is thus determined by the time-dependent correlation functions and the imposed stress perturbation. We are interested here only in the static equilibrium response a long time after the perturbation is switched on. The time-dependent strain correlation functions (computed for the unperturbed Hamiltonian $\mathcal{H} = \mathcal{H}_0$ at switched off external perturbation $\Delta\mathcal{H}$) must, of course, vanish

$$c_{\alpha\beta\gamma\delta}(\mathbf{q}, t) \to 0 \text{ for } t \to \infty. \quad (30)$$

Hence, eqn (29) reduces to

$$\delta\varepsilon_{\alpha\beta}(\mathbf{q}) = \beta V c_{\alpha\beta\gamma\delta}(\mathbf{q})\delta\sigma_{\gamma\delta}(\mathbf{q}) \text{ for } t \to \infty \quad (31)$$

with $\delta\varepsilon_{\alpha\beta}(\mathbf{q}) \equiv \lim_{t\to\infty} \delta\varepsilon_{\alpha\beta}(\mathbf{q}, t)$ denoting the long-time creep and $c_{\alpha\beta\gamma\delta}(\mathbf{q}) \equiv \lim_{t\to0} c_{\alpha\beta\gamma\delta}(\mathbf{q}, t)$ standing for the spatial correlation function without time lag, eqn (1), as everywhere else in this paper.

C. Response to point source

Following the discussion at the end of Section II, we investigate now the long-time creep for a point source

$$\delta\sigma_{\alpha\beta}(\mathbf{r}) = s_{\alpha\beta}\delta(\mathbf{r}) \quad (32)$$

with $s_{\alpha\beta}$ being a symmetric 2×2 matrix (of dimension "stress × volume = energy"). According to the FDT relation eqn (31) this implies

$$\delta\varepsilon_{\alpha\beta}(\mathbf{q}) = \beta c_{\alpha\beta\gamma\delta}(\mathbf{q})s_{\gamma\delta} \text{ for } t \to \infty \qquad (33)$$

and an equivalent relation in real space. As in Section IID it is convenient to diagonalize $s_{\alpha\beta}$ by an appropriate rotation of the coordinate system. The perturbation becomes therefore equivalent to that of two small force dipoles[23] oriented along the eigenvectors. The real-space analogue of eqn (10) is thus given by

$$\delta\varepsilon_{\alpha\beta}(\mathbf{r}) = \beta c_{\alpha\beta 11}(\mathbf{r})s_{11} + \beta c_{\alpha\beta 22}(\mathbf{r})s_{22}. \qquad (34)$$

Using in addition eqn (D13) we may replace for isotropic systems the real space correlation functions by the corresponding invariants $\tilde{i}_n(r)$ in real space. Introducing the scalars $s_1 = s_{\gamma\gamma}/2$ and $s_2 = \hat{r}_\alpha s_{\alpha\beta}\hat{r}_\beta/2$ this may be written quite generally

$$
\begin{aligned}
\delta\varepsilon_{\alpha\beta}(\mathbf{r}) &= 2\left[\tilde{i}_1(r)s_1 + \tilde{i}_3(r)s_2\right]\delta_{\alpha\beta} \\
&\quad + 2\left[\tilde{i}_3(r)s_1 + \tilde{i}_4(r)s_2\right]\hat{r}_\alpha\hat{r}_\beta \\
&\quad + 2\tilde{i}_2(r)s_{\alpha\beta}.
\end{aligned}
\qquad (35)
$$

Taking now advantage of the specific results for strain correlations presented in Section IVC and in Appendix D the invariants $\tilde{i}_n(r)$ are given by eqn (D14), *i.e.* we may quite generally express $\delta\varepsilon_{\alpha\beta}(\mathbf{r})$ in terms of the two creep compliances J_1 and J_2, *cf.* eqn (19).

We also note that the term $s_{\alpha\beta}$ in the last line of eqn (35) must be isotropic, *i.e.* $s_1 = s_{11} = s_{22} = 2s_2$, to obtain an isotropic second-order tensor field in agreement with eqn (A20). As expected from the more general argument given in Section 2, the shear strain increment

$$\delta\varepsilon_{12}(\mathbf{r})/s_{11} = -\frac{J_2}{4\pi r^2}\sin(2\theta) \text{ for } r > 0 \qquad (36)$$

becomes quadrupolar in this case.

As already emphasized in Section IIE, the source tensor need not necessarily be isotropic albeit the system is isotropic. To be specific, let us consider the "shear transformation zone" model for localized plastic failure involving two orthogonal force dipoles of opposite signs.[23] Hence, $s_{11} = -s_{22}$ and $s_1 = 0$ and $s_2 = s_{11}(\hat{r}_1{}^2 - \hat{r}_2{}^2)/2$. Using eqn (13) or eqn (35) this yields

$$\delta\varepsilon_{12}(\mathbf{r})/s_{11} = -\frac{2J_1}{4\pi r^2}\sin(4\theta) \text{ for } r > 0 \qquad (37)$$

for the shear strain response.

As one expects on general grounds, all reference to statistical physics, *i.e.* the inverse temperature β, drops out in both cases. Moreover, the shear strain response naturally strongly depends on the type of source term applied at the origin: for force dipoles of same sign it is quadrupolar and proportional to J_2 while for dipoles of opposite sign it gets octupolar and proportional to J_1.

VI. Conclusion

A. Summary

Strain correlation functions. The present work has focused on correlation functions of components of strain tensor fields in two-dimensional, isotropic and achiral elastic bodies. This was done theoretically using

● the general mathematical structure of isotropic tensor fields as summarized in Section IIB, *cf.* eqn (5), and in more detail in Appendix A and

● the well-known equipartition theorem of statistical physics for macroscopic strain fluctuations in reciprocal space, *cf.* eqn (2).

Numerically we have tested our predictions by means of glass-forming particles deep in the glass regime. This shows that these correlation functions may depend on the coordinates of the field variable (q_α in reciprocal space or r_α in real space) and implies in turn that they depend in general on the direction of the field vector and on the orientation of the coordinate system. Scaling with $x = \theta - \alpha$ these angular dependencies are distinct from those of ordinary anisotropic systems. Importantly, correlation functions of strain tensor fields are components of an isotropic forth-order tensor field, eqn (5), being characterized by the two ICFs $c_L(q)$ and $c_T(q)$. With the asymptotic plateau values being given by two Lamé coefficients, eqn (2), all strain correlation functions are determined and all (finite) real-space strain correlations must be long-ranged decaying as $1/r^2$ (*cf.* Fig. 5). We thus obtain similar results as in our recent study on correlation functions of stress tensor fields.[4] Note that time-averaged stress fields have been probed in the latter study while correlations of instantaneous strain fields have been considered here. Our numerical findings do agree with other studies of strain correlations[29,30,32] being, however, now traced back to the isotropy of the system and the tensor field nature of the probed correlations. Importantly, we have given here a complete and asymptotically exact description for the correlation functions of strain tensor fields of isotropic elastic bodies. No additional physical assumption is thus needed (for sufficiently small wavevectors).

Response to tensorial point sources. We also discussed the associated linear response fields as defined in general mathematical terms by the tensorial contraction of the correlation function tensor by means of a source tensor and, more physically, by the FDT relation for the strain increment due to an imposed small stress perturbation, *cf.* eqn (28) and (29). Naturally, the response must by definition contain information from both the correlation functions, characterizing the system, and from the imposed source tensor which may not be isotropic. We have emphasized that the summation over repeated indices must be properly performed, *i.e.* the response field is not given by one correlation function times a scalar but by the sum over all eigenvalues of the source tensor. For this reason response and correlation fields, albeit closely related, have in general different angular dependences, *e.g.*, the shear strain correlation function $c_{1212}(\mathbf{r})$ in an isotropic system must be octupolar, *cf.* eqn (25), while the shear strain response $\delta\varepsilon_{12}(\mathbf{r})$ may be

either quadrupolar for an isotropic source, *cf.* eqn (36), or octupolar for an anisotropic source corresponding to two force dipoles of opposite signs, *cf.* eqn (37). Albeit all contributing correlation functions are isotropic the response field is anisotropic in the latter case due to the source. It is thus important to not lump together correlation functions and response fields. Mesoscopic elasto-plastic models[45,46] thus must specify not only the correlation functions but also the source tensors characterizing the local plastic events.

B. Outlook

Our work suggests several natural extensions:

• The general mathematical framework for isotropic tensor fields and the discussed relations and numerical procedure for correlation and response fields naturally generalize to higher spatial dimensions, especially for the three-dimensional case.

• The present work has focused on Euclidean spaces and Cartesian coordinates. A generalization for systems embedded in non-Euclidean spaces, say for glasses on spheres,[51,52] and more general curvilinear coordinate systems[1,5] may be worked out.

• The present work has focused on the large-wavelength limit ($q \to 0$). More generally, one may express the longitudinal and transverse ICFs $c_L(q)$ and $c_T(q)$ for finite q as

$$\beta V c_L(q) = \frac{1}{L(q)} \text{ and } \beta V c_T(q) = \frac{1}{4G(q)} \qquad (38)$$

in terms of the generalized longitudinal and transverse elastic moduli $L(q)$ and $G(q)$ (with $L(q) \to \lambda + 2\mu$ and $G(q) \to \mu$ for small q).¶ [17,48,50] It can be shown[50] that both the isotropicity and the harmonicity of the strain modes assumed in the derivation of eqn (38) are well justified for the present model up to $q \approx 1$ while deviations become relevant for larger wavevectors, especially around the main peak of the static structure factor $S(q)$.

• A further generalization of the current work concerns time-dependent correlation functions $c_{\alpha\beta\gamma\delta}(\mathbf{q}, t)$ as defined in eqn (27). These can be again expressed *via* eqn (5) in terms of (now time-dependent) longitudinal and transverse ICFs $c_L(q, t)$ and $c_T(q, t)$. These time-dependent ICFs are given in turn by time-dependent creep compliance material functions which can be related to the two time-dependent material functions $L(q, t)$ and $G(q, t)$.[17] Strain correlation functions may thus reveal octupolar pattern whenever the invariant

$$|i_4(q, t)| = |c_L(q, t) - 4c_T(q, t)| \qquad (39)$$

¶ The elastic modulus tensor $E_{\alpha\beta\lambda\delta}(\mathbf{q})$ for isotropic bodies at finite wavevector $\mathbf{q}$ is not only characterized by the longitudinal modulus $L(\mathbf{q})$ and the shear modulus $G(q)$ but also by a third modulus $M(q)$ called the "mixed modulus".[17] Note that $E^\circ_{1111}(q) = E^\circ_{2222}(q) = L(q)$, $E^\circ_{1212}(q) = G(q)$ and $E^\circ_{1122}(q) = M(q)$ for isotropic bodies in NRC. It is not possible to determine $M(q)$ solely using strain fluctuations. This requires the additional measurement of stress fields in NRC. $M(q)$ may then be obtained using either the appropriate stress–strain or stress–stress correlation functions in reciprocal space.[17,50]

is sufficiently large. Since $i_4(q, t)$ must become q-independent for small q, a long-range decay with

$$c_{\alpha\beta\gamma\delta}(\mathbf{r}, t) \backsimeq 1/r^d \qquad (40)$$

is generally expected for the time-dependent correlation functions in isotropic d-dimensional systems. Using eqn (29) similar long-range relations are predicted for the associated dynamical response fields.

• It may be also of interest to characterize correlations of tensor fields of different order. For instance, the forth-order elastic modulus field $E_{\alpha\beta\gamma\delta}(\mathbf{r})$[26,53] may be characterized by a correlation function tensor of order eight.[53] Strong angular dependencies are expected based on our formalism. For isotropic systems these correlation functions must again adopt a general mathematical structure in terms of a small finite number of ICFs. Once these ICFs are characterized (theoretically or numerically using NRC) in the low-q limit all correlation functions are again determined.

Author contributions

J. P. W. designed and wrote the project benefitting from contributions of all co-authors.

Conflicts of interest

There are no conflicts to declare.

Appendix A Summary of isotropic tensor fields

1 Background

Isotropic systems are described by "isotropic tensors" and "isotropic tensor fields". We give here a brief recap of various useful aspects already presented elsewhere.[3,4] Quite generally, a tensor field assigns a tensor to each point of the mathematical space, in our case a d-dimensional Euclidean vector space.[3] We denote an element of this vector space by the "spatial position" $\mathbf{r}$ (real space) or by the "wavevector" q for the corresponding reciprocal space. The relations for tensor fields are formulated in reciprocal space since this is more convenient both on theoretical and numerical grounds due to the assumed spatial homogeneity ("translational invariance"). The corresponding real space tensor field is finally obtained by inverse FT.

For simplicity we assume Cartesian coordinates with an orthonormal basis $\{\mathbf{e}_1, \ldots, \mathbf{e}_d\}$.[1,3,9] Greek letters α, β, ... are used for the indices of the tensor (field) components. A twice repeated index α is summed over the values $1, \ldots, d$, *e.g.*, $\mathbf{q} = q_\alpha \mathbf{e}_\alpha$ with q_α standing for the vector coordinates. This work is chiefly concerned with tensors $\mathbf{T}^{(o)} = T_{\alpha_1 \ldots \alpha_o} \mathbf{e}_{\alpha_1} \ldots \mathbf{e}_{\alpha_o}$ of "order" $o = 2$ and $o = 4$ and their corresponding tensor fields with components depending either on $\mathbf{r}$ or $\mathbf{q}$. The order of a component is given by the number of indices. Note that

$$T_{\alpha_1 \ldots \alpha_o}(\mathbf{q}) = [T_{\alpha_1 \ldots \alpha_o}(\mathbf{r})] \qquad (A1)$$

for the d^o coordinates in real and reciprocal space (with $\mathcal{F}[\ldots]$ denoting the FT as discussed in Appendix B).

We consider linear orthogonal coordinate transformations (marked by "*") $\mathbf{e}_\alpha^* = c_{\alpha\beta}\mathbf{e}_\beta$ with matrix coefficients $c_{\alpha\beta}$ given by the direction cosine $c_{\alpha\beta} \equiv \cos(\mathbf{e}_\alpha^*, \mathbf{e}_\beta)$.[3] We remind that[3]

$$T_{\alpha_1\ldots\alpha_o}^*(\mathbf{q}) = c_{\alpha_1\nu_1} \ldots c_{\alpha_o\nu_o} T_{\nu_1\ldots\nu_o}(\mathbf{q}) \tag{A2}$$

under a general orthogonal transform. For a reflection of the 1-axis we thus have, *e.g.*,

$$T_{1222}^*(\mathbf{q}) = -T_{1222}(\mathbf{q}), \; T_{1221}^*(\mathbf{q}) = T_{1221}(\mathbf{q}), \tag{A3}$$

i.e. we have sign inversion for an odd number of indices equal to the index of the inverted axis. The field vector $\mathbf{q} = q_\alpha\mathbf{e}_\alpha = q_\alpha^*\mathbf{e}_\alpha^*$ remains unchanged by these "passive" transforms albeit its coordinates change.

2 Definitions, properties and construction of general isotropic tensors and tensor fields

Isotropic tensors. Components of an isotropic tensor remain unchanged by *any* orthogonal coordinate transformation,[3,9] *i.e.*

$$T_{\alpha_1\ldots\alpha_o}^* = T_{\alpha_1\ldots\alpha_o}. \tag{A4}$$

As noted at the end of Section A1 the sign of tensor components change for a reflection at one axis if the number of indices equal to the inverted axis is odd. Consistency with eqn (A4) implies that *all tensor* components with an odd number of equal indices must vanish, *e.g.*,

$$T_{12} = T_{1112} = T_{1222} = 0. \tag{A5}$$

Isotropic tensor fields. The corresponding isotropy condition for tensor fields is given by[3]

$$T_{\alpha_1\ldots\alpha_o}^*(q_1,\ldots,q_d) = T_{\alpha_1\ldots\alpha_o}(q_1^*,\ldots,q_d^*) \tag{A6}$$

with $q_\alpha^* = c_{\alpha\beta}q_\beta$ which reduces to eqn (A4) for $\mathbf{q} = \mathbf{0}$. Please note that the fields on the left handside of eqn (A6) are evaluated with the original coordinates of the vector field variable $\mathbf{q}$ while the fields on the right handside are evaluated with the transformed coordinates. Another way to state this is to say that the left hand fields are computed at the original vector $\mathbf{q} = (q_1,\ldots,q_d)$ while the right hand fields are computed at the "actively transformed" vector $q^* = (q_1^*,\ldots,q_d^*)$. It is for this reason that finite components with an odd number of equal indices, *e.g.*, $T_{1222}(\mathbf{q}) \neq 0$, are possible in principle for finite $\mathbf{q}$.

Natural rotated coordinates. Fortunately, there is a convenient coordinate system where the nice symmetry eqn (A5) for isotropic tensors can be also used for isotropic tensor fields. In these "Natural Rotated Coordinates" (NRC) the coordinate system for each wavevector $\mathbf{q}$ is rotated until the 1-axis coincides with the $\mathbf{q}$-direction, *i.e.* $q_\alpha^\circ = q\delta_{1\alpha}$ with $q = |q|$. These tensor field components in NRC are marked by "$\circ$" to distinguish them from standard rotated tensor fields (marked by primes "'") where the same rotation is used for all $\mathbf{q}$. If in addition $T_{\alpha_1\ldots\alpha_o}^\circ(\mathbf{q})$ is an even function of its field variable $\mathbf{q}$ (as in the case of achiral systems for even order o) it can be shown[4]

that all tensor field components with an odd number of equal indices must vanish.

Product theorem for isotropic tensor fields. Let us consider a tensor field $\mathbf{C}(\mathbf{q}) = \mathbf{A}(\mathbf{q}) \otimes \mathbf{B}(\mathbf{q})$ with $\mathbf{A}(\mathbf{q})$ and $\mathbf{B}(\mathbf{q})$ being two isotropic tensor fields and $\otimes$ standing either for an outer product, *e.g.* $c_{\alpha\beta\gamma\delta}(\mathbf{q}) = A_{\alpha\beta}(q)B_{\gamma\delta}(q)$, or an inner product, *e.g.* $c_{\alpha\beta\gamma\delta}(\mathbf{q}) = A_{\alpha\beta\gamma\nu}(\mathbf{q})B_{\nu\delta}(\mathbf{q})$. Hence,

$$\begin{aligned}\mathbf{C}^*(\mathbf{q}) &= (\mathbf{A}(\mathbf{q}) \otimes \mathbf{B}(\mathbf{q}))^* = A^*(\mathbf{q}) \otimes B^*(\mathbf{q}) \\ &= \mathbf{A}(\mathbf{q}^*) \otimes \mathbf{B}(\mathbf{q}^*) = \mathbf{C}(\mathbf{q}^*)\end{aligned} \tag{A7}$$

using in the second step a general property of tensor (field) products, due to eqn (A2), and in the third step eqn (A6) for the fields $\mathbf{A}(\mathbf{q})$ and $\mathbf{B}(\mathbf{q})$ where $\mathbf{q}^*$ stands for the "actively" transformed field variable. $\mathbf{C}(\mathbf{q})$ is thus also an isotropic tensor field. One may use this theorem to construct isotropic tensor fields from known isotropic tensor fields $\mathbf{A}(\mathbf{q})$ and $\mathbf{B}(\mathbf{q})$.

3. Summary of assumed symmetries

All second-order tensors in this work are symmetric, $T_{\alpha\beta} = T_{\beta\alpha}$, and the same applies for the corresponding tensor fields in either $\mathbf{r}$- or $\mathbf{q}$-space. This is, *e.g.*, the case for the strain field $\varepsilon_{\alpha\beta}(\mathbf{q}) = \mathcal{F}[\varepsilon_{\alpha\beta}(\mathbf{r})]$, *cf.* eqn (14), or the source tensor $s_{\alpha\beta}$ needed for a response field, *cf.* eqn (8). We assume for all forth-order tensor fields that

$$T_{\alpha\beta\gamma\delta}(\mathbf{q}) = T_{\beta\alpha\gamma\delta}(\mathbf{q}) = T_{\alpha\beta\delta\gamma}(\mathbf{q}) \tag{A8}$$

$$T_{\alpha\beta\gamma\delta}(\mathbf{q}) = T_{\gamma\delta\alpha\beta}(\mathbf{q}) \tag{A9}$$

and

$$T_{\alpha\beta\gamma\delta}(\mathbf{q}) = T_{\alpha\beta\gamma\delta}(-\mathbf{q}). \tag{A10}$$

Note that eqn (A10) is necessarily valid both for achiral and chiral two-dimensional isotropic systems. Forth-order tensor fields are often constructed by taking outer products[9] of second-order tensor fields. We consider, *e.g.*, correlation functions $\langle \hat{T}_{\alpha\beta}(\mathbf{q})\hat{T}_{\gamma\delta}(-\mathbf{q})\rangle$ with $\hat{T}_{\alpha\beta}(\mathbf{q})$ being an instantaneous second-order tensor field. eqn (A8) then follows from the symmetry of the second-order tensor fields. The evenness of forth-order tensor fields, eqn (A10), is a necessary condition for achiral systems. It implies that $T_{\alpha\beta\gamma\delta}(\mathbf{q})$ is real if $T_{\alpha\beta\gamma\delta}(\mathbf{r})$ is real and, moreover, eqn (A9) for correlation functions since

$$\langle \hat{T}_{\alpha\beta}(\mathbf{q})\hat{T}_{\gamma\delta}(-\mathbf{q})\rangle = \langle \hat{T}_{\gamma\delta}(\mathbf{q})\hat{T}_{\alpha\beta}(-\mathbf{q})\rangle. \tag{A11}$$

As already emphasized, all our systems are assumed to be isotropic, *i.e.*, eqn (A6) must hold for ensemble-averaged tensor fields.

4. General mathematical structure

General structure of tensors. Isotropic tensors of different order are discussed, *e.g.*, in Section 2.5.6 of ref. 9. Due to eqn (A5) all such tensors of odd order must vanish. The finite isotropic tensors of lowest order are thus

$$T_{\alpha\beta} = k_1\delta_{\alpha\beta}, \tag{A12}$$

$$T_{\alpha\beta\gamma\delta} = i_1\delta_{\alpha\beta}\delta_{\gamma\delta} + i_2(\delta_{\alpha\gamma}\delta_{\beta\delta} + \delta_{\alpha\delta}\delta_{\beta\gamma}) \tag{A13}$$

with k_1, i_1 and i_2 being invariant scalars. Please note that all symmetries stated above hold, especially also eqn (A5). Note that the symmetry eqn (A8) was used for the second relation, eqn (A13). Importantly, this implies that only *two* coefficients are needed for a forth-order isotropic tensor. As a consequence, the elastic modulus tensor is completely described by two elastic moduli (*cf.* Section 9.3).

General structure of tensor fields. We restate now the most general isotropic tensor fields for $1 \leq o \leq 4$ and focusing on two-dimensional systems ($d = 2$) compatible with the symmetries stated in Section 7.3. With $l_n(q)$, $k_n(q)$, $j_n(q)$ and $i_n(q)$ being invariant scalar functions of $q = |\mathbf{q}|$ we have[3,4]

$$T_\alpha(\mathbf{q}) = l_1(q)\hat{q}_\alpha \tag{A14}$$

$$T_{\alpha\beta}(\mathbf{q}) = k_1(q)\delta_{\alpha\beta} + k_2(q)\hat{q}_\alpha\hat{q}_\beta \tag{A15}$$

$$T_{\alpha\beta\gamma}(\mathbf{q}) = j_1(q)\hat{q}_\alpha\delta_{\beta\gamma} + j_2(q)\hat{q}_\beta\delta_{\alpha\gamma} + j_3(q)\hat{q}_\gamma\delta_{\alpha\beta} + j_4(q)\hat{q}_\alpha\hat{q}_\beta\hat{q}_\gamma \tag{A16}$$

$$\begin{aligned}
T_{\alpha\beta\gamma\delta}(\mathbf{q}) &= i_1(q)\delta_{\alpha\beta}\delta_{\gamma\delta} \\
&\quad + i_2(q)\left(\delta_{\alpha\gamma}\delta_{\beta\delta} + \delta_{\alpha\delta}\delta_{\beta\gamma}\right) \\
&\quad + i_3(q)\left(\hat{q}_\alpha\hat{q}_\beta\delta_{\gamma\delta} + \hat{q}_\gamma\hat{q}_\delta\delta_{\alpha\beta}\right) \\
&\quad + i_4(q)\hat{q}_\alpha\hat{q}_\beta\hat{q}_\gamma\hat{q}_\delta
\end{aligned} \tag{A17}$$

for finite wavevectors $\mathbf{q}$. See ref. 4 for a derivation, generalizations for $d > 2$ and a discussion of the limit $q \to 0$. Terms due to the invariants $k_1(q)$, $i_1(q)$ and $i_2(q)$ are independent of the coordinate system. All other terms depend on the components $\hat{q}_\alpha$ of the normalized wavevector $\hat{\mathbf{q}}$ and thus on the orientations of the field vector and of the coordinate system.

Alternative representation for forth-order tensor fields.

It is convenient to define the four functions

$$\left.\begin{aligned}
c_L(q) &\equiv T^\circ_{1111}(\mathbf{q}) \\
c_T(q) &\equiv T^\circ_{1212}(\mathbf{q}) \\
c_N(q) &\equiv T^\circ_{2222}(\mathbf{q}) \\
c_\perp(q) &\equiv T^\circ_{1122}(\mathbf{q})
\end{aligned}\right\} \text{ for } q^\circ_\alpha = q\delta_{1\alpha} \tag{A18}$$

using NRC. For an isotropic system these four functions can only depend on the wavenumber q but not on the direction $\hat{\mathbf{q}}$ of the wavevector $\mathbf{q}$. Importantly, all other components $T^\circ_{\alpha\beta\gamma\delta}(\mathbf{q})$ are either by eqn (A8) and (A9) identical to these invariants or must vanish for an odd number of equal indices as reminded in Section A2. The $d^4 = 16$ components $T^\circ_{\alpha\beta\gamma\delta}(\mathbf{q})$ are thus completely determined by the four invariants and this for

any q. $T_{\alpha\beta\gamma\delta}(\mathbf{q})$ is then obtained by the inverse rotation to the original unrotated frame using eqn (A2). It is readily seen that

$$\begin{aligned}
c_L(q) &= i_1(q) + 2i_2(q) + 2i_3(q) + i_4(q) \\
c_N(q) &= i_1(q) + 2i_2(q) \\
c_\perp(q) &= i_1(q) + i_3(q) \\
c_T(q) &= i_2(q)
\end{aligned} \tag{A19}$$

being consistent with eqn (6).

Isotropic tensor fields in real space. We have formulated above all tensor fields in terms of the wavevector $\mathbf{q}$ and its components since it is most convenient to start the analysis in reciprocal space. The above results also hold, however, in real space. This implies, *e.g.*, for isotropic (and achiral) fields in two dimensions that

$$T_{\alpha\beta}(\mathbf{r}) = \tilde{k}_1(r)\delta_{\alpha\beta} + \tilde{k}_2(r)\hat{r}_\alpha\hat{r}_\beta \tag{A20}$$

$$\begin{aligned}
T_{\alpha\beta\gamma\delta}(\mathbf{r}) &= \tilde{i}_1(r)\delta_{\alpha\beta}\delta_{\gamma\delta} \\
&\quad + \tilde{i}_2(r)\left[\delta_{\alpha\gamma}\delta_{\beta\delta} + \delta_{\alpha\delta}\delta_{\beta\gamma}\right] \\
&\quad + \tilde{i}_3(r)\left[\hat{r}_\alpha\hat{r}_\beta\delta_{\gamma\delta} + \hat{r}_\gamma\hat{r}_\delta\delta_{\alpha\beta}\right] \\
&\quad + \tilde{i}_4(r)\hat{r}_\alpha\hat{r}_\beta\hat{r}_\gamma\hat{r}_\delta
\end{aligned} \tag{A21}$$

for $r > 0$ with $\tilde{k}_n(r)$ and $\tilde{i}_n(r)$ denoting the invariants in real space and $\hat{r}_\alpha = r_\alpha/r$ components of the normalized vector $\hat{\mathbf{r}} = \mathbf{r}/r$. As already stated, eqn (A1), the tensor field components in real and reciprocal space are related by FT. Note that $\tilde{k}_n(r)$ and $\tilde{i}_n(r)$ are in general not the FTs of, respectively, $k_n(q)$ and $i_n(q)$. For the important case that the invariants in reciprocal space are q-independent constants it follows quite generally that

$$\begin{aligned}
4\pi r^2 \tilde{k}_1(r) &= 2k_2 \\
4\pi r^2 \tilde{k}_2(r) &= -4k_2 \\
4\pi r^2 \tilde{i}_1(r) &= 4i_3 + 5i_4 \\
4\pi r^2 \tilde{i}_2(r) &= -i_4 \\
4\pi r^2 \tilde{i}_3(r) &= -4i_3 - 6i_4 \\
4\pi r^2 \tilde{i}_4(r) &= 8i_4
\end{aligned} \tag{A22}$$

for $r > 0$. (Additional $\delta(\mathbf{r})$-terms arise at the origin. The constant invariants k_1, i_1 and i_2 only contribute to these terms.) That this holds can be readily shown using relations put forward in Appendix B and Appendix D.

Appendix B: Useful Fourier transformations

1. Continuous Fourier transform

We consider real-valued functions $f(\mathbf{r})$ in d dimensions. As in ref. 4, 18 and 54 the Fourier transform (FT) $f(\mathbf{q}) = \mathcal{F}[f(\mathbf{r})]$ from

"real space" (variable $\mathbf{r}$) to "reciprocal space" (variable $\mathbf{q}$) is defined by

$$f(\mathbf{q}) = \frac{1}{V}\int d\mathbf{r}\, f(\mathbf{r}) \exp(-i\mathbf{q}\cdot\mathbf{r}) \tag{B1}$$

with V being the volume of the system. The inverse FT is then given by

$$f(\mathbf{r}) = \mathcal{F}^{-1}[f(\mathbf{q})] = \frac{V}{(2\pi)^d}\int d\mathbf{q}\, f(\mathbf{q}) \exp(iq\cdot\mathbf{r}). \tag{B2}$$

Note that $f(\mathbf{r})$ and $f(\mathbf{q})$ have the same dimension. For notational simplicity the function names remain unchanged. We remind the FTs

$$\mathcal{F}\left[\frac{\partial}{\partial r_\alpha} f(\mathbf{r})\right] = iq_\alpha f(\mathbf{q}) \tag{B3}$$

$$\mathcal{F}[\delta(\mathbf{r} - \mathbf{v})] = \frac{1}{V}\exp(-i\mathbf{q}\cdot\mathbf{v}) \tag{B4}$$

with $\delta(\mathbf{r})$ being Dirac's delta function. Let us consider the spatial convolution function

$$f(\mathbf{r}) = \frac{1}{V}\int d\mathbf{r}'\, g(\mathbf{r} - \mathbf{r}') h(\mathbf{r}') \tag{B5}$$

in real space. With $g(\mathbf{q}) = \mathcal{F}[g(\mathbf{r})]$ and $h(\mathbf{q}) = \mathcal{F}[h(\mathbf{r})]$ this implies according to the "convolution theorem"[55]

$$f(\mathbf{q}) = \mathcal{F}[f(\mathbf{r})] = g(\mathbf{q})h(\mathbf{q}). \tag{B6}$$

We also remind for completeness that the spatial correlation function

$$c(\mathbf{r}) = \frac{1}{V}\int d\mathbf{r}'\, g(\mathbf{r} + \mathbf{r}') h(\mathbf{r}') \tag{B7}$$

of real-valued fields $g(\mathbf{r})$ and $h(\mathbf{r})$ becomes according to the "correlation theorem"[55]

$$c(\mathbf{q}) = g(\mathbf{q})h^\star(\mathbf{q}) = g(\mathbf{q})h(-\mathbf{q}) \tag{B8}$$

with $\star$ marking the conjugate complex. For auto-correlation functions, i.e. for $g(\mathbf{r}) = h(\mathbf{r})$, this simplifies to ("Wiener–Khinchin theorem")

$$c(\mathbf{q}) = g(\mathbf{q})g(\mathbf{q}) = |g(\mathbf{q})|^2, \tag{B9}$$

i.e. the Fourier transformed auto-correlation functions are real and ≥ 0 for all $\mathbf{q}$. Moreover, we shall consider correlation functions $c(\mathbf{r})$, eqn (B7), being even in real space, $c(\mathbf{r}) = c(-\mathbf{r})$, and thus also in reciprocal space, $c(\mathbf{q}) = c(-\mathbf{q}) = c^\star(\mathbf{q})$, i.e. $c(\mathbf{q})$ is real.

2. Discrete Fourier transform on microcell grid

All fields $f(\mathbf{r})$ are stored on a regular equidistant d-dimensional grid as shown in Fig. 2 for $d = 2$. Periodic boundary conditions are assumed.[33] The discrete FT and its inverse become

$$f(\mathbf{q}) = \frac{1}{n_V}\sum_{\mathbf{r}} f(\mathbf{r}) \exp(-i\mathbf{q}\cdot\mathbf{r}) \tag{B10}$$

$$f(r) = \sum_{\mathbf{q}} f(\mathbf{q}) \exp(i\mathbf{q}\cdot\mathbf{r}) \tag{B11}$$

with $\sum_{\mathbf{r}}$ and $\sum_{\mathbf{q}}$ being discrete sums over $n_V = n_L^d = V/a_{grid}^d$ grid points in, respectively, real or reciprocal space. As shown in Fig. 2 we label the grid points in real and reciprocal space using

$$\frac{r_\alpha}{a_{grid}} = n_\alpha \text{ and } q_\alpha a_{grid} = \frac{2\pi}{n_L}n_\alpha$$

$$\text{with } n_\alpha = -\frac{n_L}{2} + 1, \ldots, 0, 1, \ldots, \frac{n_L}{2}. \tag{B12}$$

To take advantage of the Fast-Fourier transform (FFT) routines[55] the number of grid points in each spatial direction $n_L = L/a_{grid}$ is an integer-power of 2.

3. Fourier transform of planar harmonic functions

As discussed in the main part, all correlation functions in reciprocal space become in the large-wavelength limit independent of the magnitude q of the wavevector $\mathbf{q}$ but depend on its angle θ_q (and, more generally, on the angle difference $\theta_q - \alpha$ for rotated coordinate frames). As noted in Section IIC, these angular dependencies can be uniquely expressed in terms of the planar harmonic basis functions $\cos(p\theta_q)$ and $\sin(p\theta_q)$ with p being an integer. We denote these orthogonal basis functions by $b_p(\theta_q)$. We thus need to compute the inverse FTs of $f(\mathbf{q}) = b_p(\theta_q)/V$. More specifically, we are interested in modes with $p = 2$ and $p = 4$. Additional constant terms ($p = 0$), such as the ones indicated by dots in eqn (20)–(22), are irrelevant leading merely to $\delta(\mathbf{r})$-contributions at the origin. For $d = 2$ eqn (B2) becomes

$$f(\mathbf{r}) = \frac{1}{4\pi^2}\int_0^\infty dq\, q \times$$
$$\int_0^{2\pi} d\theta_q b_p(\theta_q) \exp[iqr\cos(\theta_q - \theta_r)] \tag{B13}$$

with θ_r being the angle of $\hat{\mathbf{r}} = (\cos(\theta_r), \sin(\theta_r))$. We make now the substitution $\theta = \theta_q - \theta_r$ and use that[56]

$$\cos(p\theta + p\theta_r) + \cos(-p\theta + p\theta_r) = 2\cos(p\theta)\cos(p\theta_r)$$

$$\sin(p\theta + p\theta_r) + \sin(-p\theta + p\theta_r) = 2\cos(p\theta)\sin(p\theta_r).$$

We remind that following eqn (9.1.21) of ref. 56 the integer Bessel function $J_p(z)$ may be written

$$J_p(z) = \frac{i^{-p}}{\pi}\int_0^\pi d\theta\, \cos(p\theta) \exp[iz\cos(\theta)] \tag{B14}$$

which leads to

$$f(\mathbf{r}) = \frac{i^p}{2\pi}b_p(\theta_r)\int_0^\infty dq\, q J_p(rq). \tag{B15}$$

For finite r we may rewrite this as

$$f(\mathbf{r}) = \frac{i^p p}{2\pi r^2}b_p(\theta_r) \times \lim_{t\to\infty} I_p(t) \text{ for } r > 0 \tag{B16}$$

where we have set $I_p(t) \equiv \int_0^t dt' t' J_p(t')/p$. As may be seen from eqn (11.4.16) of ref. 56 the latter integral becomes‖

$$I_p(t) \to 1 \text{ for } t \to \infty \text{ and } p > -2 \qquad (B17)$$

from which we obtain the final result

$$f(\mathbf{r}) = \frac{i^p p}{2\pi r^2} b_p(\theta_r) \text{ for } r > 0. \qquad (B18)$$

Note that $f(\mathbf{r}) = f(-\mathbf{r})$ and that $f(\mathbf{r})$ is real for even p. Generalizing the above argument it is seen that $f(\mathbf{r}) \propto 1/r^d$ for higher dimensions d.

Appendix C Computational details

1 Simulation model

We consider systems of polydisperse Lennard-Jones (pLJ) particles in $d = 2$ dimensions where two particles i and j of diameter D_i and D_j interact by means of a central pair potential[4,18,36–39,48]

$$u(s) = 4\varepsilon\left(\frac{1}{s^{12}} - \frac{1}{s^6}\right) \text{ with } s = \frac{r}{(D_i + D_j)/2} \qquad (C1)$$

being the reduced distance according to the Lorentz rule.[34] This potential is truncated and shifted[4,33] with a cutoff $s_{\text{cut}} = 2s_{\text{min}}$ given by the minimum s_{min} of $u(s)$. Lennard-Jones units[33] are used throughout this study, i.e. $\varepsilon = 1$ and the average particle diameter is set to unity. The diameters are uniformly distributed between 0.8 and 1.2. We also set Boltzmann's constant $k_{\text{B}} = 1$ and assume that all particles have the same mass $m = 1$. The last point is irrelevant for the presented Monte Carlo (MC) simulations.[33] Time is measured in units of MC steps (MCS) throughout this work.

2. Parameters and configuration ensembles

We focus on systems with $n = 10\,000$ and $n = 40\,000$ particles. We first equilibrate = 200 independent configurations c at a high temperature $T = 0.55$ in the liquid limit. These configurations are adiabatically cooled down using a combination of local MC moves[33] and swap MC moves exchanging the sizes of pairs of particles.[38,49] In addition, an MC barostat[33] imposes an average normal stress $P = 2$.[36,38] At the working temperature $T = 0.2$ we first thoroughly temper over $\Delta\tau = 10^7$ all configurations with switched-on local, swap and barostat MC moves and then again over $\Delta\tau = 10^7$ with switched-on local and swap moves and switched-off barostat moves. The final production runs are

‖ The infinite integral eqn (11.4.16) of ref. 56 is expressed in terms of two coefficients μ and ν which in our case take the (real) values $\mu = 1$ and $\nu = p$. It is stated that eqn (11.4.16) holds for $\Re(\mu + \nu) > -1$, being consistent with the condition $p > -2$ noted in eqn (B17), but also that $\Re\mu < 1/2$, being at first sight in conflict with $\mu = 1$. However, the integral divergence for $t \to \infty$ for $\mu > 1/2$ is fictitious as, e.g., discussed in the Wikipedia entry on "Oscillatory integrals" where it is noted that "Oscillatory integrals make rigorous many arguments that, on a naive level, appear to use divergent integrals". Note that eqn. (B18) also holds for $p = 0$ and finite $r > 0$ which follows from the fact that the FT of a constant is zero everywhere except at the origin. See ref. 4 for an alternative more straight-forward but also more lengthy derivation of eqn. (B18) using the asymptotic behavior of the confluent hypergeometric Kummer function $M(a, b, z)$.

carried out at constant volume V only keeping local MC moves. Under these conditions, $T = 0.2$ is well below the glass transition temperature $T_{\text{g}} \approx 0.26$ determined in previous work.[36,38] Due to the barostat used for the cooling the box volume $V = L^d$ differs slightly between different configurations c while V is identical for all frames t of the time-series of the same configuration c. In all cases the number density is of order unity. For each particle number n and each of the independent configurations c we store ensembles of time series containing = 10\,000 instantaneous "frames" t. These are obtained using the equidistant time intervals $\delta\tau = 1000$ for $n = 10\,000$ and $\delta\tau = 100$ for the other system sizes.

3. Macroscopic linear elastic properties

The amorphous glasses formed by pLJ particle systems at a pressure $P = 2$ and a temperature $T = 0.2 \ll T_{\text{g}} \approx 0.26$ are for sampling (production) times $\Delta\tau \leq 10^7$ MCS reversible linear elastic bodies whose plastic rearrangements can be neglected for all practical purposes.[18,21,36,38,57,58] Moreover, these systems can be shown to be isotropic above distances corresponding to a couple of particle diameters.[18,38] Following eqn (A13) the forth-order elastic modulus tensor for isotropic systems may be written[8,9]
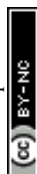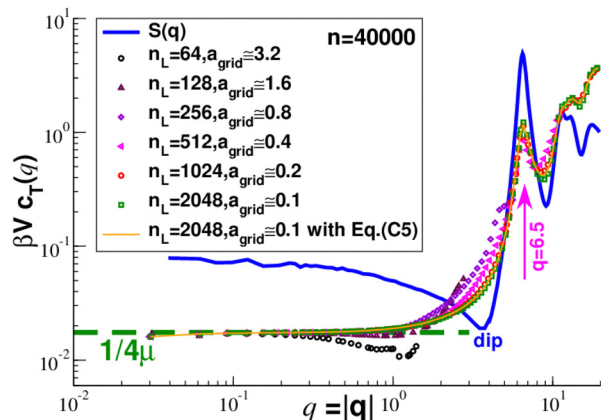
$$E_{\alpha\beta\gamma\delta} = \lambda\delta_{\alpha\beta}\delta_{\gamma\delta} + \mu(\delta_{\alpha\gamma}\delta_{\beta\delta} + \delta_{\alpha\delta}\delta_{\beta\gamma}) \qquad (C2)$$

in terms of the two isothermic Lamé moduli λ and μ. As described in detail elsewhere[21,36,57–60] we have determined λ and μ either by means of strain fluctuations, e.g., by letting the box volume V fluctuate at imposed pressure P,[57] or using the stress-fluctuation formalism at fixed volume and shape of the simulation box.[59,60] This shows that $\lambda \approx 38$ and $\mu \approx 14$. We have verified especially that similar values are obtained for $n \geq 5000$ and using different components, say E_{1111} and E_{2222} for $\lambda + 2\mu$, and that the fluctuations of $E_{\alpha\beta\gamma\delta}|_c$ for independent configurations c become negligible for $n \geq 5000$.

4. Discrete fields on square grid

We turn now to the relevant microscopic tensor fields as functions of either the spatial position $\mathbf{r}$ (real space) or the wavevector $\mathbf{q}$ (reciprocal space). The different fields are stored on equidistant discrete grids as sketched in Fig. 2. The same n_{L} is used for both spatial directions and for all configurations and frames of a given particle number n. As already mentioned, the box volume $V = L^2$ fluctuates slightly between different configurations c (at same n) due to the barostat used for the cooling, tempering and equilibration of the systems. Accordingly, a_{grid} also differs between different configurations c. These fluctuations become small, however, with increasing system size. If nothing else is mentioned we report data obtained using a lattice constant $a_{\text{grid}} \approx 0.2$. As shown in Fig. 6 for the rescaled transverse ICF $\beta V c_{\text{T}}(q)$ plotted using a double-logarithmic representation, there is no need to further decrease a_{grid}. Even the very large grid constant $a_{\text{grid}} \approx 3.2$ gives, apparently, the correct large-wavelength asymptote $\beta c_{\text{T}}(q) \approx 1/4\mu$ indicated by the dashed horizontal line.

Fig. 6 Rescaled transverse ICF $\beta V c_T(q)$ for different grid constants a_{grid} as indicated. The open symbols have been obtained using eqn (C4), the thin solid line using eqn (C5) and $n_L = 2048$. Importantly, we obtain the same results in all cases where $q u_{rms} \ll 1$ and $q a_{grid} \ll 1$. Even a rather coarse grid, say for $n_L = 64$, is sufficient to confirm the expected large-wavelength limit (horizontal dashed line). The total static structure factor $S(q)$ is shown for comparison (solid line). The "dip" of $S(q)$ around $q \approx 4$ is caused by the polydispersity of the particles as emphasized elsewhere.[48] $S(q)$ and $\beta V c_T(q)$, at least for sufficiently small a_{grid}, have both a strong peak located similarly at $q \approx 6.5$ (arrow).

5. Displacement fields

As in previous experimental and numerical studies[10,11,21] the displacement field $\mathbf{u}(\mathbf{r})$ is constructed from the instantaneous spatial positions $\mathbf{r}_a$ of the particles a with respect to their reference positions $\mathbf{r}_a$. As reference position $\mathbf{r}_a$ we have used either the average particle position determined using a long trajectory or the particle position after a rapid quench to $T = 0$. Having not observed any significant quantitative difference between both methods we only report here data computed using the first one. We thus get first the displacement vector $\mathbf{u}_a = \mathbf{r}_a - \mathbf{r}_a$ for each a. By construction the average displacement vector $\langle \mathbf{u}_a \rangle$ must vanish. We find

$$u_{rms} \equiv \langle \mathbf{u}_a^2 \rangle >^{1/2} \approx 0.13 \tag{C3}$$

for the root-mean-squared average u_{rms} (sampled over all particles, frames and configurations). The instantaneous displacement field may then be defined by[10,11,21]

$$\mathbf{u}(\mathbf{r}) = \frac{1}{n/V} \sum_a \mathbf{u}_a \delta(\mathbf{r} - \tilde{\mathbf{r}}_a) \tag{C4}$$

assuming for the moment an infinitessimal fine grid, *i.e.* $a_{grid} \to 0$. (Different prefactors have been used in ref. 10, 11 and 21). We remind that the $\delta(\mathbf{r})$-function has the dimension "1/volume". By definition $\mathbf{u}(\mathbf{r})$ has thus the same dimension "length" as the displacement vector $\mathbf{u}_a$. Following the common definition of the particle flux density,[34] the reference position $\tilde{\mathbf{r}}_a$ in the δ-function may be replaced by the time-dependent position $\mathbf{r}_a$, *i.e.* the displacement field may alternatively be defined by

$$\mathbf{u}(\mathbf{r}) = \frac{1}{n/V} \sum_a \mathbf{u}_a \delta(\mathbf{r} - \tilde{\mathbf{r}}_a). \tag{C5}$$

Both operational definitions are compared for the transverse ICF $\beta V c_T(q)$ in Fig. 6 where data obtained using eqn (C4) are indicated by open symbols. In reciprocal space we obtain

$$\mathbf{u}(\mathbf{q}) = \frac{1}{n} \sum_a \mathbf{u}_a \exp(-i\mathbf{q} \cdot \tilde{\mathbf{r}}_a). \tag{C6}$$

for eqn (C4) and similarly for eqn (C5) with $\mathbf{r}_a$ replacing $\tilde{\mathbf{r}}_a$. Since $\mathbf{r}_a = \tilde{\mathbf{r}}_a + \mathbf{u}_a$ we have to leading order

$$\exp(-i\mathbf{q} \cdot \mathbf{r}_a) \approx \exp(-i\mathbf{q} \cdot \mathbf{r}_a)(1 - i\mathbf{q} \cdot \mathbf{u}_a \ldots) \tag{C7}$$

for $q|\mathbf{u}(\mathbf{q})| \ll 1$. Both operational definitions eqn (C4) and (C5) thus become equivalent for $q u_{rms} \ll 1$. Due to the small typical (root-mean-squared) displacement u_{rms}, eqn (C3), this holds for all sampled q as may be seen from the data presented in Fig. 6. Due to the center-of-mass convention for all particle displacements the volume integral over $\mathbf{u}(\mathbf{r})$ must vanish and, equivalently, we have $\mathbf{u}(\mathbf{q} = 0) = 0$ in reciprocal space for each instantaneous field. We also remind that the two coordinates of the displacement field in NRC are the longitudinal component $u_L(q) \equiv u_1^\circ(\mathbf{q})$ and the transverse component $\mathbf{u}_T(\mathbf{q}) \equiv u_2^\circ(\mathbf{q})$.

In numerical practice, the continuous field vector $\mathbf{r}$ of eqn (C4) and (C5) corresponds to the discrete point on the grid, eqn (B12), closest (using the minimal image convention) to, respectively, the reference position $\mathbf{r}_a$ or the particle position $\mathbf{r}_a$. Strictly speaking, we thus obtain by means of eqn (B10) the FT with respect to their respective closest grid points. (In principle one could directly without approximation compute the displacement field $\mathbf{u}(\mathbf{q})$ using eqn (C6) in reciprocal space. Unfortunately, this leads to an additional loop over all n particles for each wavevector $\mathbf{q}$.) The differences between these definitions become neglible for $q a_{grid} \ll 1$. That this holds can be clearly seen from Fig. 6 where we have varied a_{grid} over more than one order of magnitude.

6. Linear strain fields

Using the displacement field $\mathbf{u}(\mathbf{r})$ the linear ("small") strain tensor field is defined by[8,9]

$$\varepsilon_{\alpha\beta}(\mathbf{r}) \equiv \frac{1}{2}\left(\frac{\partial u_\alpha(\mathbf{r})}{\partial r_\beta} + \frac{\partial u_\beta(\mathbf{r})}{\partial r_\alpha}\right). \tag{C8}$$

Due to eqn (B3) this becomes

$$\varepsilon_{\alpha\beta}(\mathbf{q}) = \frac{i}{2}\left(q_\beta u_\alpha(\mathbf{q}) + q_\alpha u_\beta(\mathbf{q})\right) \tag{C9}$$

in reciprocal space as already stated in Section IIIB. (Obviously, $\varepsilon_{\alpha\beta} = \varepsilon_{\beta\alpha}$ for any $\mathbf{r}$ in real space and any $\mathbf{q}$ in reciprocal space.) Note that both $\varepsilon_{\alpha\beta}(\mathbf{r})$ and its FT $\varepsilon_{\alpha\beta}(\mathbf{q})$, *cf.* eqn (B1), are dimensionless fields. Due to our definitions and conventions the macroscopic strain $\varepsilon_{\alpha\beta}(\mathbf{q} = 0)$ is assumed to vanish. Using eqn (B12) we numerically determine the relevant components of the (symmetric) strain tensor field $\varepsilon_{\alpha\beta}(\mathbf{q})$ from the two components of the displacement field $u_\alpha(\mathbf{q})$ stored on the reciprocal space grid (*cf.* Fig. 2) and the wavevector q_α according to eqn (B12). As noted in Section IIIB, in NRC there are only two non-vanishing strain fields, namely the longitudinal and

transverse strain fields $\varepsilon_L(\mathbf{q})$ and $\varepsilon_T(\mathbf{q})$ linearly related to the corresponding displacement fields $u_L(\mathbf{q})$ and $u_T(\mathbf{q})$, *cf.* eqn (16) and (17).

7 Correlation function fields

Using the strain tensor fields $\varepsilon_{\alpha\beta}(\mathbf{q})$ in reciprocal space computed according to eqn (C9) for each c and t we obtain the correlation functions $c_{\alpha\beta\gamma\delta}(\mathbf{q}) = \langle \varepsilon_{\alpha\beta}(\mathbf{q})\varepsilon_{\gamma\delta}(-\mathbf{q})\rangle$ averaged over all c and t. For the reported correlation functions $c'_{\alpha\beta\gamma\delta}(\mathbf{q}) = \langle \varepsilon'_{\alpha\beta}(\mathbf{q})\varepsilon'_{\gamma\delta}(-\mathbf{q})\rangle$ in a coordinate system turned by an angle α we first compute the new components $u'_\alpha(\mathbf{r})$ and q'_α of displacement field and wavevector. (Alternatively, one may also rotate $\varepsilon_{\gamma\delta}(\mathbf{q})$.) For the ICFs $c_L(\mathbf{q})$ and $c_T(\mathbf{q})$ obtained using NRC we first get the longitudinal and transverse displacement fields $u_L(\mathbf{q})$ and $u_T(\mathbf{q})$ in NRC and from those using eqn (16) and (17) the longitudinal and transverse strains $\varepsilon_L(\mathbf{q})$ and $\varepsilon_T(\mathbf{q})$. $c_L(\mathbf{q}) = \langle \varepsilon_L(\mathbf{q})\varepsilon_L(-\mathbf{q})\rangle$ and $c_T(\mathbf{q}) = \langle \varepsilon_T(\mathbf{q})\varepsilon_T(-\mathbf{q})\rangle$ are computed by averaging over all c and t and all wavevectors $\mathbf{q}$ with magnitude $|\mathbf{q}|$ within a chosen bin around $\mathbf{q}$. The correlation functions $c_{\alpha\beta\gamma\delta}(\mathbf{r})$ in real space (either for unrotated or α-rotated coordinate systems) are finally obtained by inverse FFT.

Appendix D: From $c_L(q)$ and $c_T(q)$ to $c_{\alpha\beta\gamma\delta}(r)$

As shown in Appendix A4, a forth-order tensor field describing an isotropic achiral system in two dimensions is given by eqn (A17) in terms of four invariants $i_n(q)$. In turn these invariants are expressed in terms of the alternative set of invariants $c_L(q)$, $c_T(q)$, $c_N(q)$ and $c_T(q)$. Due to eqn (18) we have $c_N(q) = c_\perp(q) = 0$ for strain correlations. The correlation function $c_{\alpha\beta\gamma\delta}(\mathbf{q})$ in reciprocal space are thus given by the invariants

$$-\frac{i_1(q)}{2} = \frac{i_3(q)}{2} = i_2(q) = c_T(q) \tag{D1}$$

and

$$i_4(q) = c_L(q) - 4c_T(q). \tag{D2}$$

More specifically, this implies

$$
\begin{aligned}
c_{1111}(\mathbf{q}) &= c^4 c_L(q) + 4s^2 c^2 c_T(q) \\
c_{2222}(\mathbf{q}) &= s^4 c_L(q) + 4s^2 c^2 c_T(q) \\
c_{1122}(\mathbf{q}) &= c^2 s^2 c_L(q) - 4s^2 c^2 c_T(q) \\
c_{1212}(\mathbf{q}) &= c^2 s^2 c_L(q) + (c^2 - s^2)^2 c_T(q) \\
c_{1112}(\mathbf{q}) &= c^3 s c_L(q) - 2sc(c^2 - s^2) c_T(q) \\
c_{1222}(\mathbf{q}) &= cs^3 c_L(q) + 2sc(c^2 - s^2) c_T(q)
\end{aligned}
\tag{D3}
$$

with $c = \cos(\theta) = \hat{q}_1$ and $s = \sin(\theta) = \hat{q}_2$ being coefficients depending only on the wavevector angle θ. Alternatively, the six relations eqn (D3) may also be obtained using that the components $\varepsilon_{\alpha\beta}(\mathbf{q})$ in the original coordinate frame can be expressed as

$$
\begin{aligned}
\varepsilon_{11}(\mathbf{q}) &= c^2 \varepsilon^\circ_{11}(\mathbf{q}) + s^2 \varepsilon^\circ_{22}(\mathbf{q}) - 2sc\,\varepsilon^\circ_{12}(\mathbf{q}) \\
&= c^2 \varepsilon_L(\mathbf{q}) - 2sc\,\varepsilon_T(\mathbf{q})
\end{aligned}
\tag{D4}
$$

$$
\begin{aligned}
\varepsilon_{22}(\mathbf{q}) &= s^2 \varepsilon^\circ_{11}(\mathbf{q}) + c^2 \varepsilon^\circ_{22}(\mathbf{q}) + 2sc\,\varepsilon^\circ_{12}(\mathbf{q}) \\
&= s^2 \varepsilon_L(\mathbf{q}) + 2sc\,\varepsilon_T(\mathbf{q})
\end{aligned}
\tag{D5}
$$

$$
\begin{aligned}
\varepsilon_{12}(\mathbf{q}) &= sc\,\varepsilon^\circ_{11}(\mathbf{q}) - sc\,\varepsilon^\circ_{22}(\mathbf{q}) + (c^2 - s^2)\varepsilon^\circ_{12}(\mathbf{q}) \\
&= cs\,\varepsilon_L(\mathbf{q}) + (c^2 - s^2)\varepsilon_T(\mathbf{q})
\end{aligned}
\tag{D6}
$$

in terms of the longitudinal and transverse strains $\varepsilon_L(\mathbf{q})$ and $\varepsilon_T(\mathbf{q})$ and the fact that $\varepsilon_L(\mathbf{q})$ and $\varepsilon_T(\mathbf{q})$ fluctuate independently. For the correlation functions $c'_{\alpha\beta\gamma\delta}(\mathbf{q})$ in rotated coordinate systems one simply replaces θ by $x = \theta - \alpha$. Note also that $c'_{1112}(q)$ and $c'_{1222}(q)$ do in general not vanish for all x in standard (unrotated or rotated) coordinates. The values for NRC are obtained by setting $x = 0$, *i.e.* $s = 0$ and $c = 1$. We expand the angle-dependent coefficients before $c_L(q)$ and $c_T(q)$ in terms of the planar harmonic functions $\cos(p\theta)$ and $\sin(p\theta)$ with p being integers using standard trigonometric relations.[56] This implies for example

$$c_{1212} = \frac{1}{8}[(4c_T - c_L)\cos(4\theta) + (4c_T + c_L)]$$

$$c_{1122} = \frac{1}{8}[(4c_T - c_L)\cos(4\theta) - (4c_T - c_L)]$$

$$\frac{c_{1111} + c_{2222}}{2} = \frac{1}{8}[-(4c_T - c_L)\cos(4\theta) + 3c_L + 4c_T]$$

$$\frac{c_{1111} - c_{2222}}{2} = \frac{1}{4}(2c_L)\cos(2\theta)$$

where we have omitted the arguments $\mathbf{q}$ on the l.h.s. and $\mathbf{q}$ on the r.h.s. The prefactor of $\cos(4\theta)$ and $\sin(4\theta)$ is always proportional to $i_4(q)$. Having in mind the equipartition relation eqn (2) and using the creep compliances J_1 and J_2 introduced in eqn (19) one sees that

$$\beta V[4c_T(q) - c_L(q)] \to J_1 \equiv \frac{1}{\mu} - \frac{1}{\lambda + 2\mu}, \tag{D7}$$

$$\beta V[2c_L(q)] \to J_2 \equiv \frac{2}{\lambda + 2\mu} \tag{D8}$$

in the low-q limit. We thus get in reciprocal space

$$\beta V c_{1212}(\mathbf{q}) \to \frac{J_1}{8}\cos(4\theta) + \dots$$

$$\beta V c_{1122}(\mathbf{q}) \to \frac{J_1}{8}\cos(4\theta) + \dots$$

$$\beta V \frac{c_{1111}(\mathbf{q}) + c_{2222}(\mathbf{q})}{2} \to -\frac{J_1}{8}\cos(4\theta) + \dots$$

$$\beta V \frac{c_{1111}(\mathbf{q}) - c_{2222}(\mathbf{q})}{2} \to \frac{J_2}{4}\cos(2\theta)$$

where the dots mark constant terms. These terms are irrelevant for the inverse FT, only leading to contributions at $\mathbf{r} = 0$.

We may thus take advantage of the analytical result for the inverse FT eqn (B18). This leads to

$$\beta c_{1212}(\mathbf{r}) \rightarrow \frac{J_1}{4\pi r^2}\cos(4\theta) \qquad \text{(D9)}$$

$$\beta c_{1122}(\mathbf{r}) \rightarrow \frac{J_1}{4\pi r^2}\cos(4\theta) \qquad \text{(D10)}$$

$$\beta\frac{c_{1111}(\mathbf{r}) + c_{2222}(\mathbf{r})}{2} \rightarrow -\frac{J_1}{4\pi r^2}\cos(4\theta) \qquad \text{(D11)}$$

$$\beta\frac{c_{1111}(\mathbf{r}) - c_{2222}(\mathbf{r})}{2} \rightarrow -\frac{J_2}{4\pi r^2}\cos(2\theta) \qquad \text{(D12)}$$

with θ denoting the polar angle of the field vector $\mathbf{r}$. The correlation functions $c'_{\alpha\beta\gamma\delta}(\mathbf{r})$ in rotated coordinate systems generalize the above equations by substituting θ with the angle difference $x = \theta - \alpha$. These results can be rewritten compactly using the general form expected from eqn (A21) for a manifest two-dimensional, isotropic and achiral forth-order tensor field in real space yielding

$$\begin{aligned}\beta c'_{\alpha\beta\gamma\delta}(\mathbf{r}) &= \tilde{i}_1(r)\delta_{\alpha\beta}\delta_{\gamma\delta} \\ &+ \tilde{i}_2(r)\big[\delta_{\alpha\gamma}\delta_{\beta\delta} + \delta_{\alpha\delta}\delta_{\beta\gamma}\big] \\ &+ \tilde{i}_3(r)\big[\hat{r}'_\alpha\hat{r}'_\beta\delta_{\gamma\delta} + \hat{r}'_\gamma\hat{r}'_\delta\delta_{\alpha\beta}\big] \\ &+ \tilde{i}_4(r)\hat{r}'_\alpha\hat{r}'_\beta\hat{r}'_\gamma\hat{r}'_\delta\end{aligned} \qquad \text{(D13)}$$

where the invariants $\tilde{i}_n(r)$ in real space are given by

$$\begin{aligned}4\pi r^2\tilde{i}_1(r) &= J_2 - 3J_1, \\ 4\pi r^2\tilde{i}_2(r) &= J_1, \\ 4\pi r^2\tilde{i}_3(r) &= 4J_1 - J_2 \text{ and} \\ 4\pi r^2\tilde{i}_4(r) &= -8J_1.\end{aligned} \qquad \text{(D14)}$$

Since $i_1 = -(2J_1 + J_2)/4$, $i_2 = (2J_1 + J_2)/8$, $i_3 = (2J_1 + J_2)/4$ and $i_4 = -J_1$, this is consistent with the more general relation eqn (A22).
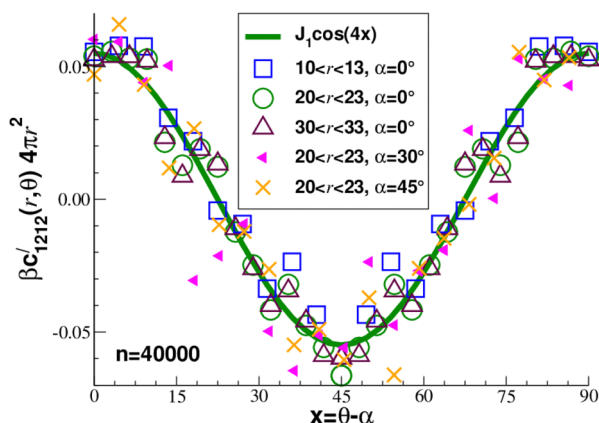

Fig. 7 Rescaled shear-strain autocorrelation function $\beta c'_{1212}(r,\theta)4\pi r^2$ in real space as a function of $x = \theta - \alpha$ comparing data for different r-intervals and rotation angles α with the prediction (bold solid line).

The angle dependence for the shear-strain autocorrelation function in real space is investigated in Fig. 7 where we plot using linear coordinates $\beta c'_{1212}(r,\theta)4\pi r^2$ as a function of x for different r and α. (To obtain sufficiently high statistics we need to average over the indicated finite r-bins. This is done by weighting each data entry for a bin with the proper factor $4\pi r^2$.) The data compare well with the prediction, eqn (D9), confirming thus especially the scaling with angle difference $x = \theta - \alpha$. Naturally, the statistics deteriorates with increasing r due to the faster decay of the correlations as compared to the noise.

Acknowledgements

References

1 A. J. McConnell, *Applications of Tensor Analysis*, *Hassell Street Press*, 2021.

2 J. A. Schouten, *Tensor Analysis for Physicists*, Dover Publications, Oxford, 2015.

3 W. Schultz-Piszachich, *Mathematik 11: Tensoralgebra und -analysis. Thun und Frankfurt/Main*, Verlag Harri Deutsch, 1977.

4 J. P. Wittmer, A. N. Semenov and J. Baschnagel, Correlations of tensor field components in isotropic systems with an application to stress correlations in elastic bodies, *Phys. Rev. E*, 2023, **108**, 015002.

5 R. J. A. Lambourne, *Relativity, Gravitation, and Cosmology*, Cambridge University Press, Cambridge, 2010.

6 T. Frankel, *The Geometry of Physics: An Introduction*, Cambridge University Press, Cambridge, 3rd edn, 2012.

7 P. M. Chaikin and T. C. Lubensky, *Principles of condensed matter physics*, Cambridge University Press, 1995.

8 L. D. Landau and E. M. Lifshitz, *Theory of Elasticity*, Pergamon Press, New York, 1959.

9 E. B. Tadmor, R. E. Miller and R. S. Elliot, *Continuum Mechanics and Thermodynamics*, Cambridge University Press, Cambridge, 2012.

10 C. Klix, F. Ebert, F. Weysser, M. Fuchs, G. Maret and P. Keim, Glass elasticity from particle trajectories, *Phys. Rev. Lett.*, 2012, **109**, 178301.

11 C. L. Klix, G. Maret and P. Keim, Discontinuous shear modulus determines the glass transition temperature, *Phys. Rev. X*, 2015, **5**, 041033.

12 M. Maier, A. Zippelius and M. Fuchs, Emergence of long-ranged stress correlations at the liquid to glass transition, *Phys. Rev. Lett.*, 2017, **119**, 265701.

13 M. Maier, A. Zippelius and M. Fuchs, Stress auto-correlation tensor in glass-forming isothermal fluids: From viscous to elastic response, *J. Chem. Phys.*, 2018, **149**, 084502.

14 F. Vogel, A. Zippelius and M. Fuchs, Emergence of Goldstone excitations in stress correlations of glass-forming colloidal dispersions, *Europhys. Lett.*, 2019, **125**, 68003.

15 A. Lemaître, Tensorial analysis of Eshelby stresses in 3d supercooled liquids, *J. Chem. Phys.*, 2015, **143**, 164515.

16 A. Lemaître, Stress correlations in glasses, *J. Chem. Phys.*, 2018, **149**, 104107.

17 L. Klochko, J. Baschnagel, J. P. Wittmer and A. N. Semenov, Long-range stress correlations in viscoelastic and glass-forming fluids, *Soft Matter*, 2018, **14**, 6835.

18 L. Klochko, J. Baschnagel, J. Wittmer, H. Meyer, O. Benzerara and A. N. Semenov, Theory of length-scale dependent relaxation moduli and stress fluctuations in glass-forming and viscoelastic liquids, *J. Chem. Phys.*, 2022, **156**, 164505.

19 D. Steffen, L. Schneider, M. Müller and J. Rottler, Molecular simulations and hydrodynamic theory of nonlocal shear stress correlations in supercooled fluids, *J. Chem. Phys.*, 2022, **157**, 064501.

20 A. Kabla and G. Debrégeas, Local Stress Relaxation and Shear Banding in a Dry Foam under Shear, *Phys. Rev. Lett.*, 2003, **90**, 258303.

21 J. P. Wittmer, H. Xu, O. Benzerara and J. Baschnagel, Fluctuation-dissipation relation between shear stress relaxation modulus and shear stress autocorrelation function revisited, *Mol. Phys.*, 2015, **113**, 2881.

22 K. W. Desmond and E. R. Weeks, Measurement of Stress Redistribution in Flowing Emulsions, *Phys. Rev. Lett.*, 2015, **115**, 098302.

23 G. Picard, A. Ajdari, F. Lequeux and L. Bocquet, Elastic consequences of a single plastic event: A step towards the microscopic modeling of the flow of yield stress fluids, *Eur. Phys. J. E: Soft Matter Biol. Phys.*, 2004, **15**, 371.

24 L. Bocquet, A. Colin and A. Ajdari, Kinetic theory of plastic flow in soft glassy materials, *Phys. Rev. Lett.*, 2009, **103**, 036001.

25 J. Chattoraj and A. Lemaître, Elastic Signature of Flow Events in Supercooled Liquids Under Shear, *Phys. Rev. Lett.*, 2013, **111**, 066001.

26 H. Mizuno, S. Mossa and J. L. Barrat, Measuring spatial distribution of the local elastic modulus in glasses, *Phys Rev E*, 2013, **87**, 042306.

27 A. Nicolas, J. Rottler and J. L. Barrat, Spatiotemporal correlations between plastic events in the shear flow of athermal amorphous solids, *Eur. Phys. J. E: Soft Matter Biol. Phys.*, 2014, **37**, 50.

28 E. Flenner and G. Szamel, Long-range spatial correlations of particle displacements and the emergence of elasticity, *Phys. Rev. Lett.*, 2015, **114**, 025501.

29 B. Illing, S. Fritschi, D. Hajnal, C. Klix, P. Keim and M. Fuchs, Strain pattern in supercooled liquids, *Phys. Rev. Lett.*, 2016, **117**, 208002.

30 M. Hassani, E. M. Zirdehi, K. Kok, P. Schall, M. Fuchs and F. Varnik, Long-range strain correlations in 3d quiescent glass forming liquids, *Europhys. Lett.*, 2018, **124**, 18003.

31 C. Liu, G. Biroli, D. R. Reichman and G. Szamel, Dynamics of liquids in the large-dimensional limit, *Phys Rev E*, 2021, **104**, 054606.

32 R. N. Chacko, F. P. Landes, G. Biroli, O. D. A. J. Liu and D. R. Reichman, Elastoplasticity Mediates Dynamical Heterogeneity Below the Mode Coupling Temperature, *Phys. Rev. Lett.*, 2021, **127**, 048002.

33 M. P. Allen and D. J. Tildesley, *Computer Simulation of Liquids*, Oxford University Press, Oxford, 2nd edon; 2017.

34 J. P. Hansen and I. R. McDonald, *Theory of simple liquids*, Academic Press, New York, 3rd edn, 2006.

35 D. Forster, *Hydrodynamic Fluctuations, Broken Symmetry, and Correlation Functions*, Perseus Books, New York, 1995.

36 J. P. Wittmer, H. Xu, P. Polińska, F. Weysser and J. Baschnagel, Shear modulus of simulated glass-forming model systems: Effects of boundary condition, temperature and sampling time, *J. Chem. Phys.*, 2013, **138**, 12A533.

37 L. Klochko, J. Baschnagel, J. P. Wittmer and A. N. Semenov, Relaxation dynamics in supercooled oligomer liquids: From shear-stress fluctuations to shear modulus and structural correlations, *J. Chem. Phys.*, 2019, **151**, 054504.

38 G. George, L. Klochko, A. N. Semenov, J. Baschnagel and J. P. Wittmer, Ensemble fluctuations matter for variances of macroscopic variables, *Eur. Phys. J. E: Soft Matter Biol. Phys.*, 2021, **44**, 13.

39 G. George, L. Klochko, A. N. Semenov, J. Baschnagel and J. P. Wittmer, Fluctuations of non-ergodic stochastic processes, *Eur. Phys. J. E: Soft Matter Biol. Phys.*, 2021, **44**, 54.

40 J. D. Ferry, *Viscoelastic properties of polymers*, John Wiley & Sons, New York, 1980.

41 M. Rubinstein and R. H. Colby, *Polymer Physics*, Oxford University Press, Oxford, 2003.

42 M. Doi and S. F. Edwards, *The Theory of Polymer Dynamics*, Clarendon Press, Oxford, 1986.

43 J. K. G. Donth, *The Glass Transition: Relaxation dynamics in liquids and disordered materials*, Springer, Berlin-Heidelberg, 2001.

44 A. Argon and H. Kuo, Plastic flow in a disordered bubble raft (an analog of a metallic glass), *Mater. Sci. Eng.*, 1979, **39**, 101.

45 D. Rodney, A. Tanguy and D. Vandembroucq, Modeling the mechanics of amorphous solids at different length scale and time scale, *Modell. Simul. Mater. Sci. Eng.*, 2011, **19**, 083001.

46 A. Nicolas, E. Ferrero, K. Martens and J. L. Barrat, Deformation and flow of amorphous solids: Insights from elasto-plastic models, *Rev. Mod. Phys.*, 2018, **90**, 045006.

47 M. L. Falk and J. S. Langer, Dynamics of viscoplastic deformation in amorphous solids, *Phys Rev E*, 1998, **57**, 7192.

48 L. Klochko, J. Baschnagel, J. P. Wittmer and A. N. Semenov, Relaxation moduli of glass-forming systems: temperature effects and fluctuations, *Soft Matter*, 2021, **17**, 7867.

49 A. Ninarello and L. Berthier, Coslovich D. Models and Algorithms for the Next Generation of Glass Transition Studies, *Phys. Rev. X*, 2017, **7**, 021039.

50 J. P. Wittmer, A. N. Semenov and J. Baschnagel Strain fluctuations at finite wavevectors for isotropic colloidal glasses using natural rotated coordinates. in preparation. 2023.

51 J. P. Vest, G. Tarjus and P. Viot, Mode-coupling approach for the slow dynamics of a liquid on a spherical substrate, *J. Chem. Phys.*, 2015, **143**, 084505.

52 F. Turci, G. Tarjus and C. P. Royall, From Glass Formation to Icosahedral Ordering by Curving Three-Dimensional Space, *Phys. Rev. Lett.*, 2017, **118**, 215501.

53 H. Mizuno and S. Mossa, *Mat Phys.*, 2019, **22**, 43604.

54 J. P. Wittmer, A. N. Semenov and J. Baschnagel, Different spatial correlation functions for non-ergodic stochastic processes of macroscopic systems, *Eur. Phys. J. E: Soft Matter Biol. Phys.*, 2022, **45**, 65.

55 W. H. Press, S. A. Teukolsky, W. T. Vetterling and B. P. Flannery, *Numerical Recipes in FORTRAN: the art of scientific computing*, Cambridge University Press, Cambridge, 1992.

56 M. Abramowitz and I. A. Stegun, *Handbook of Mathematical Functions*, Dover, New York, 1964.

57 J. P. Wittmer, H. Xu, P. Polińska, C. Gillig, J. Helfferich and F. Weysser, *et al.*, Compressibility and pressure correlations in isotropic solids and fluids, *Eur. Phys. J. E: Soft Matter Biol. Phys.*, 2013, **36**, 131.

58 J. P. Wittmer, H. Xu and J. Baschnagel, Shear-stress relaxation and ensemble transformation of shear-stress auto-correlation functions revisited, *Phys Rev E*, 2015, **91**, 022107.

59 J. F. Lutsko, Stress and elastic constants in anisotropic solids: Molecular dynamics techniques, *J. Appl. Phys.*, 1988, **64**, 1152.

60 J. F. Lutsko, Generalized expressions for the calculation of elastic constants by computer simulation, *J. Appl. Phys.*, 1989, **65**, 2991.